Implementation of a DC Microgrid

by

Lee SHAVER

A project report submitted in fulfillment of the requirements for the degree of

Masters of Science
(Electrical Engineering)

at the

UNIVERSITY OF WISCONSIN-MADISON

May 2017

This material is based in part upon work supported by the National Science Foundation under Grant Numbers IIP-1542959 and CHE-1230751, the Wisconsin Electric Machines and Power Electronics Consortium (WEMPEC), and the Baldwin Wisconsin Idea Endowment from the University of Wisconsin-Madison. Any opinions, findings, and conclusions or recommendations expressed in this material are those of the author and do not necessarily reflect the views of the National Science Foundation.

APPROVED BY:

Advisor: Giri Venkataramanan

Professor

Advisor Title

30 May 2017

Date

“Hofstadter’s Law: It always takes longer than you expect, even when you take into account Hofstadter’s Law.”

Douglas Hofstadter

Abstract

The first permanent electric grid powered only the homes and buildings in its immediate vicinity–much like microgrids, which are presently the focus of intense research and development. An area holding great promise for application of microgrids is electrification and grid improvement in the developing world. The potential of microgrids in this space is examined, and development of a system intended for this context is detailed. The Microgrid Energy Manager (MEM) system is proposed as a low-cost, scalable, modular system for quickly establishing microgrids with off-the-shelf components. Design of the system for interfacing with dc loads and sources is described, and tests of the system's ability to monitor batteries, prioritize loads, and share battery capacity between interconnected microgrids are conducted. Finally, microgrid work done in partnership with students and faculty at the National Institute of Engineering in Mysuru, India is detailed. Goals of this work include establishing a live microgrid testbed on the NIE campus, and preparation of remote villages for permanent microgrids.

Acknowledgements

"I owe it all to my parents." Your love, support, and advice over the years has given me both the confidence to take risks, and the humility to keep returning to the difficult tasks long after the glamor has worn off.

I thank my advisor, Professor Giri, for his wisdom and guidance–both as an engineer working to solve difficult problems, and as a human seeking to make the world a more livable place for all. Your example is an inspiration.

To my fellow grad students, Adria Brooks, David Selhoff, Michael Rios, Zhentao Du, Calvin Cherry; your support (both academic and moral) has been invaluable. To the entire WEMPEC team: faculty, staff, and fellow students: thank you for creating and sustaining a world-class research group.

To Ashray Manur–jack of all trades, and master of a lot of them: your constant dedication to your work is inspiring, and the humility with which you've lead the project team is indispensable. Thank you for the countless hours helping me debug everything from microcontrollers to Indian social norms.

To Professor Shamsundar Subarroa and Vikram Atreya of CREST: thank you for your indispensable support during my time in your beautiful city of Mysuru. To the faculty, staff, and students of the National Institute of Engineering, and Principal Dr. G. L. Shekar: thank you for hosting me at your institution, and for all the support you provided. I hope to visit again soon.

And to Kristy: Through your eyes I have seen that the world is both more beautiful and more fragile than I had recognized. You have inspired me to apply my skills and passions to making that world a better place, starting with my very next step…

Contents

List of Figures

List of Tables

List of Abbreviations

AGM	**A**bsorbant **G**lass **M**at
a-Si	**a**morphous **Si**licon
CAN	**C**ontroller **A**rea **N**etwork
CPL	**C**onstant **P**ower **L**oad
CREST	**C**entre for **R**enewable **E**nergy and **S**ustainable **T**echnology
DER	**D**istributed **E**nergy **R**esource
HEM	**H**omegrid **E**nergy **M**anager
HVDC	**H**igh **V**oltage **dc**
LAN	**L**ocal **A**rea **N**etwork
Li-ion	**Li**thium-**ion**
MEM	**M**icrogrid **E**nergy **M**anager
MDG	**M**illennium **D**evelopment **G**oal
MPPT	**M**aximum **P**ower **P**oint **T**racking
multi-Si	**multi**crystalline **Si**licon
NIE	**N**ational **I**nstitute of **E**ngineering
OECD	**O**rganisation for **E**conomic **C**o-operation and **D**evelopment
PV	**P**hoto**v**oltaic
RE	**R**ural **E**lectrification
RET	**R**enewable **E**nergy **T**echnology
SE4All	**S**ustainable **E**nergy for **All**
SHS	**S**olar **H**ome **S**ystem(s)
SOC	**S**tate-**o**f-**c**harge
UNF	**U**nited **N**ations **F**oundation
UPS	**U**ninterruptible **P**ower **S**upply
VRLA	**V**alve-**r**egulated **L**ead-**a**cid

List of Symbols

I_{MP}	current at maximum power	A
I_{SC}	short circuit current	A
P	real power	W
P_{max}	maximum power	W
Q	charge	Ah
S	apparent power	VA
V_{MP}	voltage at maximum power	V
V_{nom}	nominal voltage	V
V_{OC}	open circuit voltage	V

Chapter 1

Introduction

1.1 The first electric grid

FIGURE 1.1: Drawing of the Pearl Street Station in Manhattan [1]

In 1882 Thomas A. Edison's fledgling electric utility, the Edison Electric Illuminating Co, flipped the switch to on at Pearl Street Station, the world's first permanent power plant [2]. The plant consisted of six 100 kW "jumbo" dynamos, and initially served 85 customers–a number which jumped to 513 by the end of the year. Each customer, located within one kilometer of the plant, used the electricity exclusively for lighting, using bulbs purchased for $1 each (over $20 USD in 2017 dollars) from the Edison Electric Illuminating Co.

The Pearl Street Station and subsequent plants provided power at 110 V_{dc} [3]. While this system had some advantages over proposed ac systems, and served customers well initially, its chief limitation eventually resulted in its demise: with no existing technology to easily step direct current up or down, it could not be transmitted over distances much longer than a kilometer [4]. As a result, ac generation and transmission (championed by Nikola Tesla and George Westinghouse) eventually won out over dc in the famous "war of the currents."

1.2 Microgrids enter the scene

Tremendous advancements occurred over the next century: the development of induction and synchronous machines, electric meters, high voltage transmission, gas turbines, nuclear reactors, wind turbines, and solar photovoltaics, to name a few [5–7]. All of these technologies were turned to the development, advancement, and expansion of "the grid;"

the system of large-scale centralized generation connected to energy users through a network of transmission and distribution.

But while a seemingly endless supply of effort and funding was being poured into "the largest machine ever built" [8, 9], in recent years another trend in research started, as some began to explore the advantages to moving in the other direction: distributed, decentralized, local grids: microgrids (see fig. 1.2).

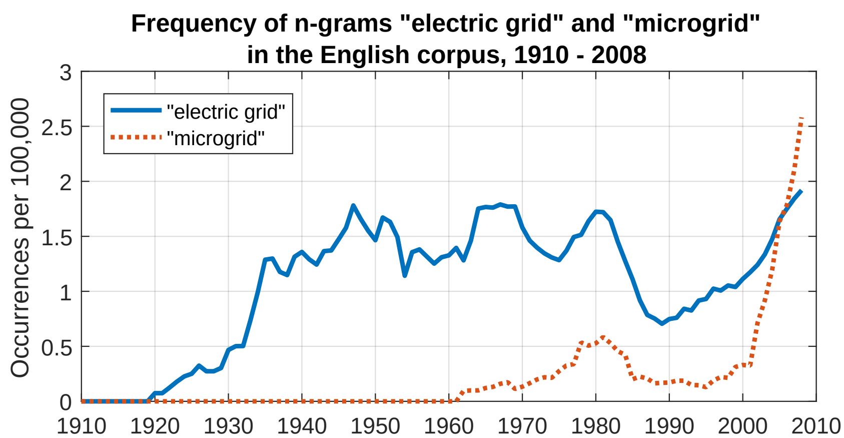

FIGURE 1.2: A chart showing the frequency of use over time of "electric grid" and "microgrid" [10, 11]

While the idea of a micro (that is, small) grid had been around for some time [12–14], researchers at UW-Madison were among the first to conceive of the microgrid in its modern form: a group of energy sources and loads, usually including storage, and an independent control system allowing for grid-connected or "islanded" operation [15, 16].

In 2012, a formal definition was provided by the U.S. Department of Energy's Microgrid Exchange Group [17]:

> A microgrid is a group of interconnected loads and distributed energy resources within clearly defined electrical boundaries that acts as a single controllable entity with respect to the grid. A microgrid can connect and disconnect from the grid to enable it to operate in both grid-connected or island-mode.

The original motivation for the idea in its early conceptions at UW-Madison was to create a framework that would allow distributed energy resources (DERs) to peacefully co-exist with the grid (see fig. 1.3) [18, 19]. Prior to work on microgrids, many utilities required customers with DERs to disconnect those resources whenever they detected an issue with the grid voltage or frequency [20, 21]. These requirements, intended to protect utility workers and other customers on the grid, created obstacles for those with such resources, making integration and control complicated and expensive, and reducing their desirability.

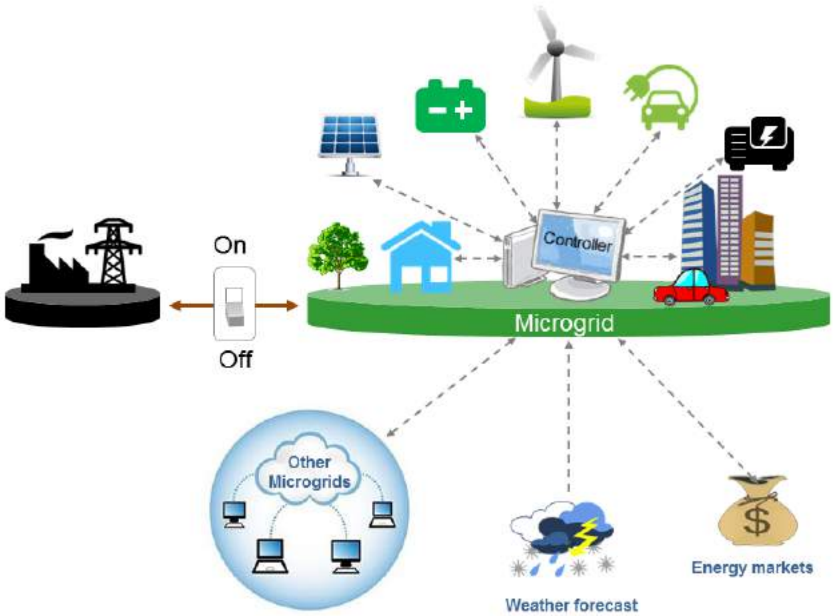

FIGURE 1.3: A conceptual schematic of a microgrid (copyright Berkeley Lab) [19]

But with a well-planned microgrid, power users would benefit from being able to aggregate a number of sources and loads under one control system, proving benefits such as back-up power, co-generation, improved power quality, and reduced environmental impact (when using renewable resources). From the utility perspective, grouping these entities under a microgrid means there are less loads and resources to keep track of and oversee. Later research also found that well-regulated microgrids are capable of providing a number of other benefits to the larger grid, including voltage and reactive power (VAR) regulation. This is an area of ongoing study–in 2009 the Electric Power Research Institute (EPRI) began development of a communications protocol for interfacing microgrids and DERs with utility systems [22], and the Institute of Electrical and Electronics Engineers (IEEE) developed a standard for interconnecting DERs with the grid [23].

1.3 Evolution of microgrid development

To date, a significant amount of microgrid development and testing has focused on large-scale microgrids, operating in spaces such as hospitals, military bases, remote villages, and government sites [24–26]. Additionally, many labs and college campuses have functional microgrids operating as part of research efforts [27–29].

In such settings, microgrids are used to accomplish a number of goals: protection from disruptions in supply (such as those due to natural disasters [30]), reducing outage time of critical loads, reducing CO_2 emissions, improving grid stability [17], and allowing seamless integration of renewables with the grid [31].

In many ways, each of those objectives can be brought back to financial motivation: added value, reduced losses, and improved returns on renewable energy systems. But even as the business case for microgrids has grown stronger [32], the advances in technology have opened up paths which are not strictly motivated by profit.

Specifically, microgrids have been envisioned as a solution to the worldwide lack of access to affordable and reliable electricity [33–35].

1.3.1 Global status of electrification

From 1990 to 2012, worldwide access to electricity increased from 75.6% to 84.6%, representing a net electrification of nearly 200 million individuals. South Asia and Sub-Saharan Africa, the regions with the lowest historical electrification rates, increased by 28% and 13%, respectively [36].

These improvements are due in large part to efforts by the the international community. In 2005, the UN commissioned a report investigating the links between lack of modern energy services (including both electricity and cooking fuels) and the Millennium Development Goals (MDGs), originally proposed in 2000, which focus on improving eight human development indicators such as poverty, gender equality, health, and education [37]. The report makes the case that without modern energy infrastructure, efforts to fully accomplish any of the goals are hampered. Following this finding, in 2012 the UN, partnering with the World Bank, launched the "Sustainable Energy For All" initiative (abbreviated SE4All, SE4ALL, or SEforALL in the literature) [38]. The goals of this project are implementing universal electricity access, doubling the share of renewables in the energy sector, and doubling the rate at which energy efficiency improves annually [39].

Along with these efforts, the World Bank and independent researchers have also investigated outcomes and best practices for rural electrification (RE). Research indicates that improvements in areas such as income inequality, poverty rates, and economic growth are not inherently a result of increasing electrification, but that carefully designed projects can bring about measurable improvements [40–43].

1.3.2 Microgrids for a new context

In addition to the benefits of increasing electrification, another key area of research seeks to identify the most cost effective means for improving electricity access. Several studies have compared outcomes for grid extension vs decentralized generation (using an average cost for all feasible sources)[44], grid extension vs solar home systems (SHS) [45], SHS vs solar photovoltaic (PV) microgrids [46], and a three-way comparison between grid extension, renewable-based home systems, and renewable-based microgrids [47].

Each of these studies analyzes some combination of transmission, distribution, fuel, and capital costs for the RE options considered.

In general, the results of these studies indicate that while grid extension is typically the least-cost option for RE, decentralized options are significantly more cost-effective in remote and/or sparsely populated areas. In particular, [44] found that in several Sub-Saharan African nations, over 50% of the population could best be served with off-grid power systems. In addition, the rapid decline of solar PV pricing over the last few years indicates that the extent of territory where SHS and PV microgrid systems are the best option will likely increase instead of decrease.

While these results might seem a somewhat under-whelming endorsement of the prospects for microgrids in developing nations, two additional factors must be considered. First, of 11 million households which were electrified by World Bank projects between 2000 and 2014, 8.7 million (roughly 80%) were connected by grid extension, 2 million (roughly 20%) by solar home system, and just over 100,000 (less than 1%) by microgrid (also called minigrid in the literature) [43]. This indicates that despite their promise, microgrids are just beginning to be utilized in RE projects. The focused research and development efforts underway around the world indicate that the growth of microgrids in this area will be rapid.

Region	**Electric outages per month**[a]	**Typical outage duration (hours)**[a]	**Population with electricity access**[b]	
			Total (%)	**Rural (%)**
South Asia	25.4	3.1	78.0	69.3
Sub-Saharan Africa	9.0	4.2	35.3	15.3
OECD countries	0.4	0.4	99.9	99.7

[a] For commercial users only
[b] For residential users only

TABLE 1.1: Grid statistics for selected regions [36, 48]

Secondly, another aspect of electric infrastructure in developing nations indicates a role for microgrids beyond electrification: the poor quality of electric connections. Table 1.1 shows grid statistics for selected regions of the world: South Asia, Sub-Saharan Africa, and for comparison, the average for nations in the Organisation for Economic Co-operation and Development (OECD), a club of rich nations.

These statistics present a dichotomy between the ways in which microgrids have been developed in rich nations, and the ways their strengths can be leveraged to meet needs in the developing world. Figure 1.4 illustrates this dichotomy: whether considering a microgrid for a hospital in New York City, or for an isolated forest village in India, individuals and organizations have the same goals; reducing costs, improving electric supply, and utilizing RETs (renewable energy technologies). But the underlying reasons guiding those choices are fundamentally different.

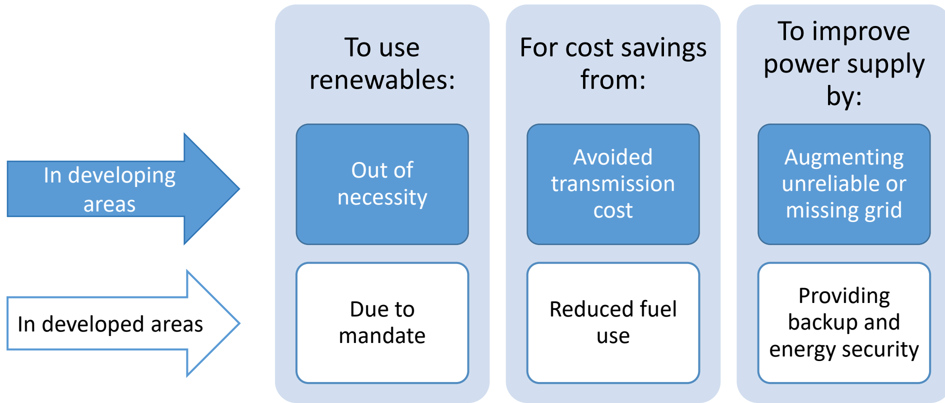

FIGURE 1.4: Motivations for installing microgrids in different contexts

For example, when building a microgrid in an urban area in the US or Europe, RETs may be more desirable than fossil-fuel burning generators due to restrictions on local pollution [49]; whereas in a remote village RETs may be the only feasible solution. Similarly, microgrids with RETs in a location where grid connection is present may represent cost savings largely due to reduced need for purchasing power from the grid, or ability to sell excess power back to the grid; whereas in remote areas, the cost of grid extension may be significantly higher than the cost of establishing a microgrid.

This dichotomy necessarily leads to differences in the design and operation of microgrids in a developing world context.

1.4 Microgrid design considerations for developing world contexts

Building on the differences in motivation identified in fig. 1.4, several guiding criteria are identified for application of microgrids in the developing world:

1. Type, availability, and cost of energy resources
2. Availability of electrical components (chargers, inverters, batteries, etc)
3. Strengths and weaknesses of existing electrical supply (if any)
4. Needs and priorities of users to be served
5. Training and ability of users to operate and maintain the system
6. Ability to adapt to expected changes in grid availability
7. Ability to adapt to changes (generally, growth) in load

Another key difference which must be considered for microgrid development is the manner in which the electric grid grows and develops. In the business as usual scenario, the grid, and thus electrification, grows outwards from places with existing reliable grid connections (such as cities and industrial areas). Communities on the edges of the grid would be electrified first, followed by their neighbors, and moving outwards (indeed, this is the paradigm used in several of the the studies cited in section 1.3.2 when comparing alternate means of electrification). At the same time, reliability and capacity of the grid in those areas already connected would increase (at least in principle).

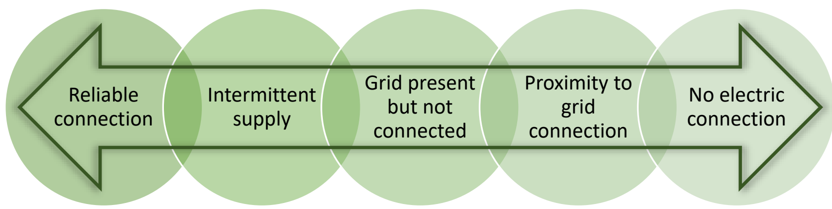

FIGURE 1.5: A bidirectional spectrum of electrification

But what if development could also flow in the opposite direction? Or better still–in both directions at the same time, as illustrated in fig. 1.5. From connected areas, the grid could continue to grow and expand outward, while simultaneously, microgrids could be used at the opposite extreme–areas far from the grid–to provide electric connections. These microgrids would introduce not only electric connections for users, but components that can eventually contribute to grid stability and reliability. Thus, when the two paradigms "meet in the middle," total power availability and reliability will be higher, at a lower cost, then if only one solution were employed.

1.5 Status of microgrids for developing world electrification

As described in [43], of 11 millions households electrified through World Bank Projects from 2000 to 2014, just over 100,000 were electrified by microgrids. But rather than representing a poor showing for microgrids, this small share represents the start of a new trend.

Challenging the assumption that centralized generation is more cost-effective than decentralized, [45] examines the possibility that developing nations could use decentralized electrification paradigms to "leapfrog" the centralized model employed elsewhere. The authors develop a model for comparing costs between centralized and decentralized electrification. While they find that off-grid systems are only likely be cost effective in about 20% of the scenarios examined, their research indicates that attributes of decentralized options such as flexibility, scalability, and rapidly falling costs mean that they are likely to become more competitive in the near future.

Further examining factors affecting adoption of microgrids, [35] discusses barriers to private sector investment in decentralized electrification projects. Specific barriers identified include unpredictable revenue, poor financing, and long-term risks. At the root of many challenges to private sector investment in microgrids for RE is that the motivation for RE is typically social in nature, making it a better fit for public and donor institutions. But several factors specific to microgrids make them an increasingly attractive option for private investment.

First, the modular nature of microgrid design means that once a base microgrid is established, adding new connections (that is, paying customers) in adjacent buildings, neighborhoods, or communities is more cost effective than in a system based on stand-alone power systems such as SHS. This, combined with the well-established trend of users to steadily increase consumption over time following initial connection, means that the prospects for long-term growth in revenue are strong for microgrids.

Second, microgrids are inherently designed to integrate with other microgrids or the main grid. This flexibility stands in contrast to stand-alone technologies, and reduces the long-term risk of "stranded assets," a situation where power systems installed for RE are rendered obsolete by the introduction of a grid connection. In such a situation, microgrids continue to offer such advantages as back-up power, improved power quality, and possible revenue from selling excess power back to the grid.

A 2014 report by the United Nations Foundation (UNF) provides case studies of seven microgrid developers operating from the 1990s through the present across India, Malaysia, and Haiti [34]. Together, these developers maintain 787 microgrids with a combined capacity of nearly 15 MW, serving nearly 60,000 customers. The UNF report categorizes microgrid business models into for profit, partially subsidized, and fully subsidized. Within these categories the authors examine seven factors which are critical to microgrid success: design of tariffs, tariff collection processes, maintenance processes, theft of service risks, growth in demand, technical limits, and local ownership and operation. Through in-depth case studies of 12 microgrids built and managed by the developers covered in the report, the authors demonstrate that careful attention must be paid to each of these seven factors to ensure the long-term success of a microgrid project.

While all of these seven factors apply to any RE technology, the technical considerations apply differently for microgrids. For instance, microgrids are much more capable of handling growth in demand and stringent technical limits, due to the modular nature of their design. Whereas an electrification project based on SHS would set a hard limit on power usage for each customer, a microgrid consisting of interconnected homes and business would have an aggregate limit for the entire community–meaning that a user with momentarily high demand could "borrow" capacity from other users with lower demand in that moment.

Finally, [50] examines issues related to microgrid deployment in India. Extending the findings from the UNF report in [34], the authors find that microgrids occupy a poorly defined middle ground between the traditional supply-side model of centralized utilities, and the simplicity of individually owned and operated systems such as solar home systems. The cooperative nature of microgrids, while resulting in improved technical performance compared to both centralized and individual systems, nonetheless brings a number of requirements (technical, legal, and financial) that are not faced by those systems. However, the government of India has recognized the benefits of microgrids, and is engaged with utilities and microgrid installers and operators to address these concerns. Two key areas of ongoing research are the development of economically sustainable ownership models, and tariff structures.

1.6 Conclusion

The development of microgrids has brought electric grid technology back to its roots: Microgrids today show significant promise as a technology for providing electric connections for communities and neighborhoods which have never before had a connection, much like the customers in the vicinity of Thomas Edison's Pearl Street Station.

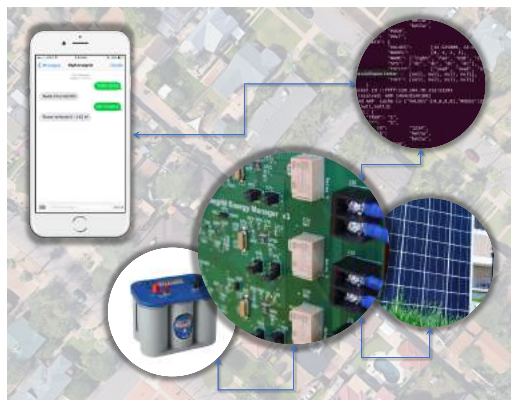

FIGURE 1.6: Graphic illustrating the components of the MEM/HEM system introduced in chapter 3

While not a panacea, electrification has the potential to positively influence development around the world, and as a result donor organizations and governments in developing nations have poured significant resources into increasing electrification. Developments in microgrid technology have presented a promising new paradigm for increasing electrification that can bypass many of the obstacles inherent in standard grid expansion (including both high capital costs and often poor reliability). In the last several decades a number of pilot projects have demonstrated the potential of microgrids not only to provide electrification in remote areas, but to do so in a way that is more resilient, cost-effective, and flexible than conventional grid expansion. From a technical perspective microgrids also mesh well with renewable energy resources, thus increasing their appeal as a more healthy and environmentally friendly option.

1.6.1 Document organization

The rest of this document is organized as follows: Chapter 2 summarizes recent trends in dc microgrid research and development. Chapter 3 gives an overview of the Microgrid Energy Manager / Homegrid Energy Manager (MEM/HEM) system being developed at UW-Madison. Chapter 4 provides details and results from two experiments conducted using the HEMdc system. Chapter 5 describes the ongoing work at the National Institute of Engineering in Mysuru, India to test the MEM system in a real-world situation. Finally, chapter 6 provides conclusions and a discussion of future work related to the efforts described in this report.

Chapter 2

Overview of dc microgrids

2.1 Introduction

As discussed in chapter 1, dc power systems have existed since the earliest days of electrical systems–but theirapplication to modern microgrids has been a more recent development. The opportunities for dc microgrids are based on three key advantages [51–54]:

Many renewable energy sources provide dc output. Solar photovoltaics and fuel cells produce dc current directly, and many wind power systems can easily produce dc current, or are interfaced to the ac grid through a dc link.

Energy storage is typically dc. Batteries and supercapacitors use dc current by their nature for charging and discharging. This includes the batteries in electrical vehicles, meaning dc power systems can easily integrate with vehicle-to-grid systems.

Many types of electrical loads use dc power natively. The majority of electronics (such as computers, servers, and TVs) use dc power. LED lights also use dc power natively. Many types of motors and drives (especially variable speed drives) use dc power.

In all three cases, these sources, storage systems, and loads require converters whenever they interface with ac power systems; thus switching to a dc power system eliminates the need for such converters, eliminating the losses which are inherent in any type of power conversion.

To date, key areas of implementation for dc power systems have included data centers, spacecraft, airplanes, shipboard power systems, traction power systems (for trains, trolleys, trams, etc), and telecommunication infrastructure. Developments in these areas have spurred research on dc microgrids, and in some cases provided test-beds for establishing functional dc microgrids (particularly in the case of data centers and telecoms, where the cost savings potential is significant).

Extending the motivations discussed in chapter 1, dc microgrids are also found to have widespread application in developing nations [55–58], due to lower electric demand,

and the suitability of solar photovoltaics in many areas. Even when higher power requirements are present, dc microgrids are still found to be well-suited in applications where a high percentage of renewable energy sources with dc output is present [58, 59].

After a brief overview of microgrid control, this chapter will cover the current status of dc microgrid research.

2.2 Three layers of microgrid control

Control systems for microgrids (whether ac, dc, or hybrid) typically consist of three control layers [60–62]. Divisions between the three layers are often defined by the time constants affecting the operation of each–from sub-seconds for primary layer, seconds to minutes for secondary control, and minutes to hours for tertiary control. The general functions of each layer are described in the following sections. A diagram illustrating how these three control layers relate to the MEM/HEM system, described in chapter 3, is provided in fig. 2.1.

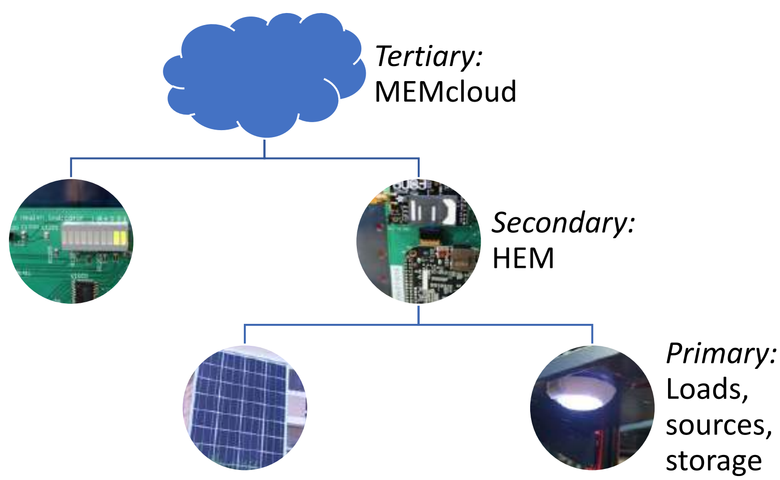

FIGURE 2.1: Illustration of the three microgrid control layers as implemented in the HEM/MEM system, introduced in chapter 3

2.2.1 Primary control

Primary control governs interaction between individual microgrid components and the larger microgrid, most often without the need for any communication interface. In the primary layer each component sets and seeks its own voltage, frequency, and power production or consumption based on local measurement. This layer is typically designed in such a way that control strategies also result in suppression of harmful harmonics and circulating currents. Responses on this layer are on the range of milliseconds. Droop control is a common strategy employed within the primary layer.

2.2.2 Secondary control

Because primary control principally governs the interaction between individual components and the larger microgrid, a secondary layer is needed to manage interactions across the microgrid between these components. The secondary layer manages holistic control within the microgrid, adjusting voltage and frequency set-points which are used by the primary layer. Secondary control typically employs a communication interface, which by design is low-bandwidth; the slower time constant of secondary control does not require high-bandwidth communication. However, several de-centralized means of employing secondary control have also been studied with some success.

2.2.3 Tertiary control

Finally, the interaction between the microgrid and the outside world is handled by the tertiary control layer. This includes deciding when to connect and disconnect from the grid, economic dispatch of power sources, load balancing and curtailment, and dispatch based on environmental and meteorological factors (particularly important for microgrids with a high share of wind and solar resources).

2.3 Status of dc microgrid research and development

2.3.1 Standardization in dc microgrids

Emerging standards and best-practices for system protection in dc microgrids are discussed in [51, 54]. The need for standards is described in terms of the key risk associated with dc power systems: arcing, fire, electrocution, and damage to loads. Key requirements for protective systems are identified as reliability, speed, performance, economics, and simplicity. Components for which standards are lacking are identified as fuses, circuit breakers, no load switches, and solid state switches. In addition to these required components, several design paradigms requiring standardization are also identified, namely: redundancy, fault isolation, load prioritization, load shedding, transient operation, and condition-based maintenance.

2.3.2 Centralized control systems

A fuzzy logic-based control system is developed and simulated in [59]. The input fuzzy variables used in the system are power balance (difference between total power produced and load power) and change in battery state-of-charge (SOC). The output variable is change in battery charge/discharge current. The system is implemented using wireless sensors and actuators connected through LabVIEW. Simulation and experimental evaluation of the system demonstrates its ability to provide stable power to loads with fluctuating input power from a wind and solar source, while simultaneously maintaining battery SOC in a desirable range, and supplying excess power back to the grid.

In [55] a centralized, rules-based system for dc microgrid control is developed and tested through simulation. The back-end of the microgrid is purely dc–all sources, loads, and storage devices are connected through ac-dc or dc-dc converters to a common dc-link at a nominal 300 V. The energy management system handles control of the MPPT interfaces for the two power sources (wind turbine and solar PV), charging/discharging of the batteries and supercapacitor used for storage, and load shedding. Data inputs consist of the dc link voltage and battery SOC. For a one second simulation including load- and source-stepping events, it is demonstrated that the proposed algorithm is able to maintain the dc link voltage within 0.04 V of the set-point.

More robust control systems which can adapt to changes in operating modes are proposed and simulated in [58, 63, 64]. Four types of terminals for dc microgrids are defined: dispatchable loads, dispatchable sources, intermittent sources, and a grid interface. Use of dc voltage measurement is proposed as a proxy for stability, and a tiered structure is constructed, where defined ranges in voltage are assumed to correspond to standard variations in operating modes of any system with each type of terminal present. The voltage tiers also correlate to the number of power versus slack buses present at any given time. Different control schemes are used within each voltage range, variously comprising droop, proportional control, proportional-integral control, feedback loops, and high- and low-pass filtering.

In [63], while the system performs well in certain aspects of controlled simulation, it is inherently reliant on careful selection of voltage parameters, and assumes uniform, constant voltage drop between any two points in the microgrid. Varying voltage measurements are accounted for in the experimental setup tested in [64], but the accuracy and reliability of the voltage measurement system is identified as a critical and costly component of the system, limiting its extensibility.

In [58], the system uses the time constant and frequency of disturbances to determine the root cause event, and implements a control strategy targeted at responding to specific, predetermined events. In simulation the system is able to distinguish between events and implement the proscribed control strategy to restore stability, but further testing with different events and simultaneous events is required.

2.3.3 Decentralized control systems

Moving in the direction of decentralized control, [65] proposes a control system where each node on the dc microgrid handles primary control locally with droop, only requires a data link to its immediate neighbors (using a graph network) for secondary and tertiary control functions. Each node transmits its own measured per-unit voltage and current, and its estimate of the network voltage. Voltage drop between nodes is accommodated by setting a communication "weight," or data transfer gain. A voltage observer with noise filtering combines the local and neighboring voltage measurements to estimate the voltage across the microgrid, and thus determine the correct local setpoint. To set initial control parameters, prior knowledge of the frequency response must be known, as well as the microgrid admittance matrix.

In simulation and an experiment using laboratory equipment, the proposed control system outperforms standard droop control in correctly maintaining the voltage setpoint and implementing load-sharing. It also demonstrates immunity to noise. Response to load changes, converter failure, and failure of individual data linkages are also tested with satisfactory results.

A decentralized approach, treating all terminals the same, is proposed and simulated by [66]. Prior attempts to develop robust secondary control for dc microgrids are found to assume presence of a single power source, neglect voltage drop between different points on the grid, or artificially insert a small ac signal to attempt "borrowing" of ac control methods.

To overcome these challenges, a decentralized, droop-based system tuned for low voltage regulation is combined with a centralized controller to ensure load sharing. The communication scheme proposed uses digital signals (to reduce the impact of noise), while only requiring transmission of two bytes of data per source–allowing for the use of robust yet low-bandwidth, low-speed networks such as CAN (controller area network). In a system with two loads and two sources, simulations and experimental evaluation demonstrate average voltage regulation less than 3%, and current sharing error below 0.5%.

2.3.4 Hybrid ac and dc microgrids

Another important consideration of dc microgrids is interoperability with ac systems [67]. A hybrid system consisting of dc interconnection to share dc sources and storage is considered in [57]. This system effectively consists of creating a shared bus for dc loads and the batteries used for storage: the bulk of the control tasks are still handled by the ac systems.

In contrast, [68] considers "pairs" of ac and dc microgrids which share a single storage system and grid-tie connection. In this system, standard primary and secondary control methods can be used for the two ac and dc "subgrids," while the tertiary controller serves as a "gatekeeper" to connect the subgrids to each other, storage, or the grid, through a common dc link. With droop control for the two subgrids, an experimental system was developed which demonstrated the system's ability, using only low-bandwidth communication, to effectively manage the two subgrids, focusing on reducing charging/discharging of batteries (increasing their lifespan) and reduced operation time of power converters (to minimize losses).

2.3.5 Control of interconnected dc microgrids

A control scheme for clusters of dc microgrids is proposed in [69]. Decentralized control at the primary level regulates voltage and current sharing using adaptive droop control based on battery SOC. At the secondary level, power flow between connected microgrids in the cluster is managed by a centralized controller adjusting voltage set-points based on the SOC within each microgrid. When a single microgrid is preparing to connect with the cluster, this secondary controller will match the dc-link voltage to allow for smooth transition; once connected, the secondary controllers of all connected microgrids cooperate to adjust voltage set-points and facilitate power flow between microgrids based on relative SOC. Similar to [65], a graph network is used to connect the controller of each microgrid and share measured voltage and SOC.

In simulation, voltage and battery charge/discharge current of individual microgrids is properly controlled, and connection between microgrids is shown to have a smooth transition. The ability of three interconnected microgrids to share power and move towards a common value for SOC (microgrids with higher charge sending charging current to those with less) is also demonstrated.

While not specific to dc microgrids, [70] also considers group control of microgrids, including economic considerations as a control factor. For a group of interconnected microgrids, when any individual microgrid has a power shortage, it can choose between consuming fuel for dispatchable energy sources (such as a generator), purchasing power from the grid, or purchasing from other microgrids. Conversely, a microgrid with excess capacity can sell this power to the grid, sell it to other microgrids, or store it (within storage limits). Each of these choices have specific economic impacts which can change seasonally, daily, or even hourly. While operation of any microgrid has economic considerations and constraints, the added option of exchange with neighboring microgrids adds an additional degree of freedom to the problem of optimal economic dispatch. This creates a more complex problem, which the authors address by solving the optimization in a piecewise linear fashion. In simulations based on an actual microgrid installation in Guangxi Province, China the proposed control method demonstrates that interconnected microgrids are able to operate in a more profitable way than an identical group of non-cooperating microgrids.

2.4 Conclusion

The nature of renewable energy sources, energy storage systems, and many typical loads provides significant potential for dc microgrids. Such microgrids are a natural outgrowth from existing development for data centers, traction power systems, and other areas where dc power systems have been used for decades. However, there remains a lack of standardization for protection and control in dc power systems.

Control in dc microgrids can be broadly separated into centralized and decentralized approaches; the former typically being more robust and stable, with the latter being easier and more cost-effective to implement. Significant effort has also been put into control systems for hybrid ac-dc microgrids, or interfaces between ac- and dc-microgrids. An additional area of research which has not received significant attention in the past is the effect of aggregating microgrids, and the benefits and challenges this could bring.

Chapter 3

MEM: Microgrid Energy Manager

3.1 Introduction

MEM, the Microgrid Energy Manager, is a platform conceived and developed at the University of Wisconsin-Madison for the purpose of microgrid research and development, in line with the priorities discussed in chapter 1. MEM involves groups of individual *homegrids* aggregated together as a microgrid. A homegrid may consist of a home or small business with its own local energy sources (typically solar PV) and storage (typically batteries). Several homegrids grouped together comprise a microgrid, which may also include shared resources such as larger energy sources (wind turbines, generators, or hydroelectric plants), street lights, and pumped water energy storage. A schematic of such a system is given in fig. 3.1.

MEM consists of two major components, and several sub-components:

MEMcloud: The Microgrid Energy Manager cloud application, which monitors and controls individual microgrids and their component homegrids.

HEM: The Homegrid Energy Manager, a hardware and software platform which performs local monitoring and control of individual homegrids. Each HEM may consists of several components:

- **HEMcore:** The core hardware required for a homegrid, including processors and communications interfaces.
- **HEMapp:** The software running on HEMcore which actively monitors and controls loads, and interfaces with MEMcloud through several possible communications protocols. This includes the firmware and drivers necessary to operate the hardware peripherals, as well as user code which makes decisions about how to operate the hardware.
- **HEMac:** Energy metering and relays used for interfacing with ac loads and sources (110 – 230 V_{ac}, 50 – 60 Hz), interfaced through third-party potential transformers, current transformers, and contactors.

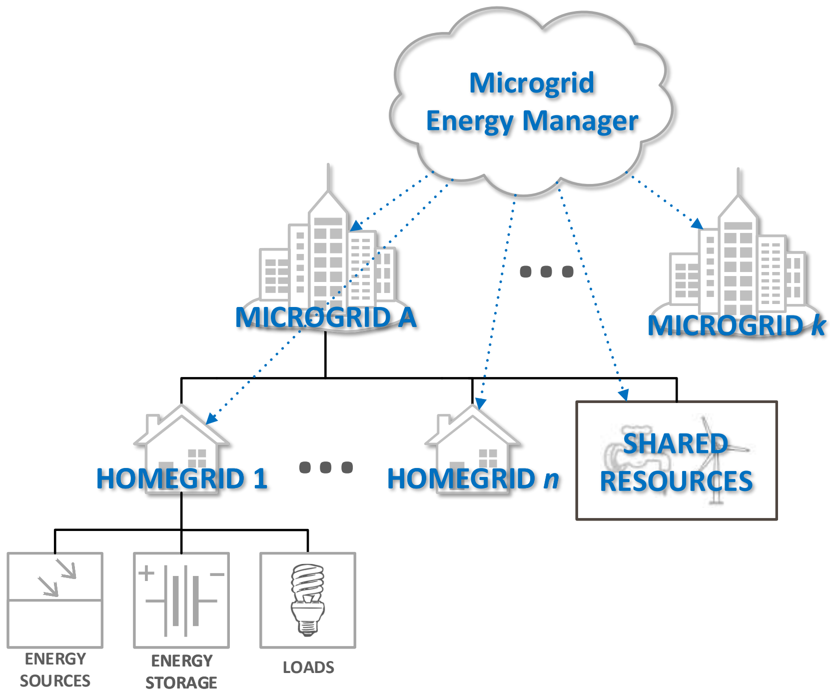

FIGURE 3.1: Illustration of MEM/HEM hierarchy [71]

HEMdc: Energy metering and relays used for interfacing with dc loads, sources, and batteries (12 – 48 V_{dc}, up to 10 A per circuit).

The relationship between these components and MEMcloud is illustrated in fig. 3.2. The rest of this chapter will provide additional details on the design and function of the MEM components, going into detail where applicable for this paper.

3.1.1 Previous publications on MEM

The MEM system has been in development since 2013, and has served as the subject of several previous papers.

In [62], a masters thesis, the wireless sensor network for establishing and monitoring MEM microgrids/homegrids is developed. Testing of reliability and network elements in various topologies and physical environments was performed. Results from this work guided the development of a hardware system which served as the immediate precursor to the MEM/HEM system which is the subject of the present study.

MEM was also the subject of several forthcoming papers presented at a conference in December 2016 [72]. Aggregation of power and storage requirements for homes is studied in [73], where a simulation of four average Wisconsin residences finds that load variability can be reduced by up to 25%, and battery storage requirements by 10%. In [71], the motivation and need for MEM system is given, highlighting gaps in current

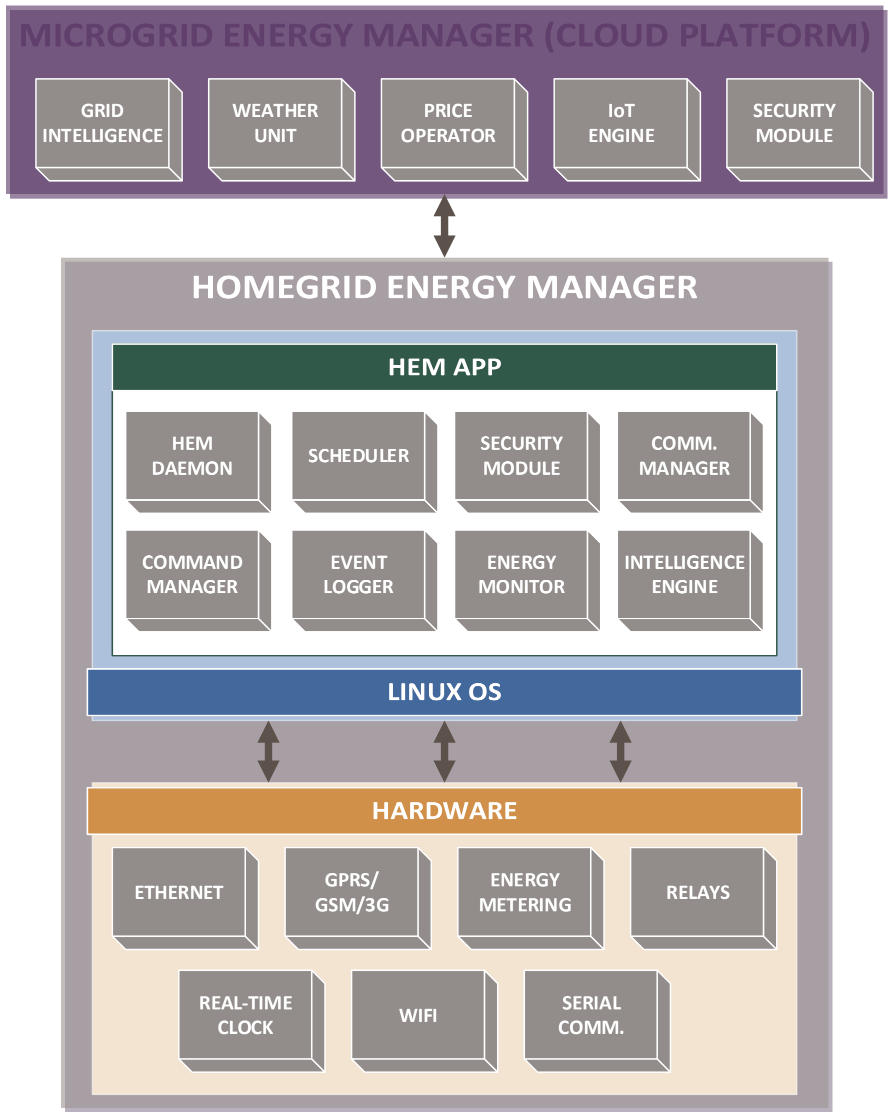

FIGURE 3.2: Block diagram of MEM and HEM components [71]

research on the topic of small-scale microgrids. Finally, [74] provides further test and verification of the wireless sensor network system developed in [62].

3.2 MEMcloud

MEMcloud is a cloud application which handles data storage, system management, and remote user interface. Long term, MEMcloud will be responsible for collecting and analyzing all data relevant to the operation of microgrids and homegrids. This includes such data as weather forecasts, solar availability predictions, fuel prices, and grid electricity costs. MEMcloud is also responsible for monitoring and controlling shared community resources which are not associated with a specific homegrid, such as large-scale energy sources and storage, as well as public services such as street lighting and water treatment.

3.3 HEM

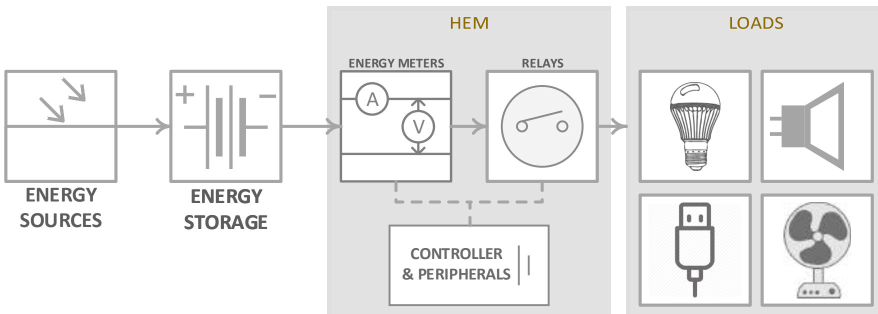

FIGURE 3.3: Example of a homegrid [71]

A homegrid is a small autonomous unit within a microgrid–typically a home or small business, with a small solar array and one or two batteries, as illustrated in fig. 3.3. Larger homegrids are also possible, but at this stage in development the focus is on systems with demands in the range of hundreds of watts.

The HEM system consists of the HEMcore hardware, paired with one or both of HEMac and HEMdc interfaces. The hardware platform is managed by the HEMapp software.

HEMapp is responsible for monitoring the battery and loads to keep the system operating within limits. HEMapp also handles communication with MEMcloud and the local user interface. The basis of HEMapp is a multi-threaded application written in C which interfaces with each of the hardware components. User applications are written in Python, which then interface with HEMapp through an on-board UDP server.

3.3.1 HEMdc interface

HEMdc was developed in early 2017 for the purpose of isolating the communications and processing components of the HEM system from the relays and energy meters which interface directly with potentially high-power loads and sources (an ac corollary, not covered in this paper, has also been developed). A block diagram of the hardware is shown in fig. 3.4.

The main features of HEMdc are:

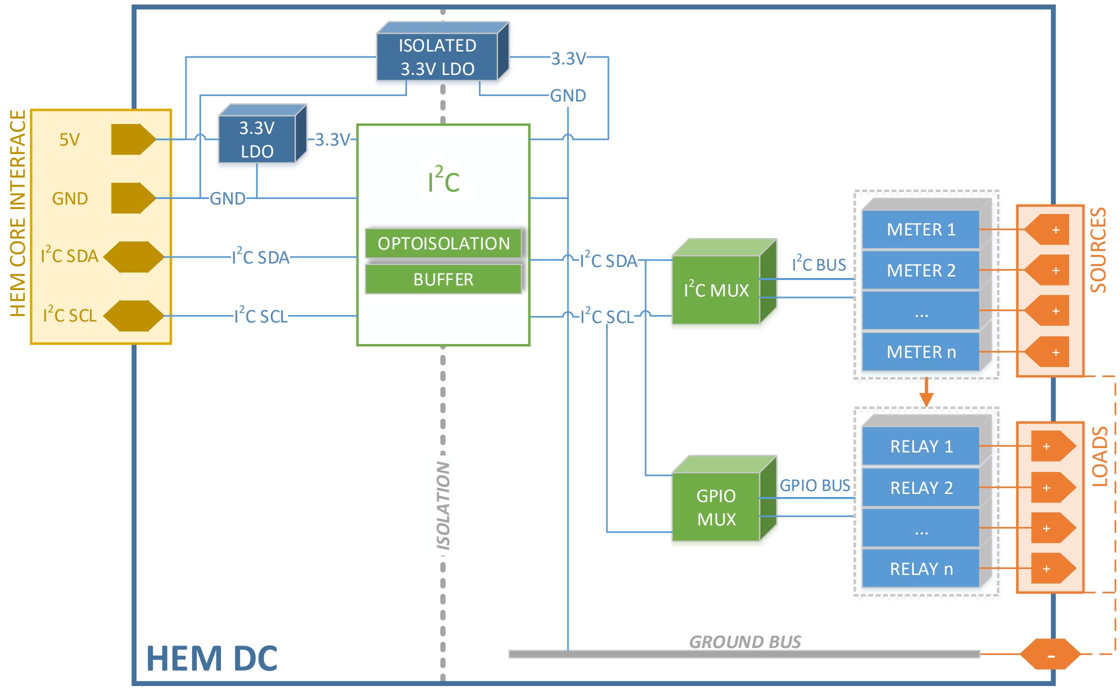

FIGURE 3.4: Block diagram of HEMdc interface

I^2C interface with isolation and buffering. HEMdc communicates with HEMcore over an I^2C interface. I^2C is a serial bus interface consisting of a serial data line and serial clock line pulled-up to 3.3 V_{dc} [75]. Because I^2C is specified for communication within a PCB, buffering and optical isolation is added to extend functionality to provide a board-to-board interface, improve reliability, and provide protection for the HEMcore components.

Isolated power supply from HEMcore. The same cable which carries the HEMcore data interface also supplies 5 V_{dc} power to operate HEMdc. The 5 V_{dc} is fed through a 1 W isolated, regulated, dc-dc converter. As with the I^2C lines, isolation is implemented to protect the HEMcore components. Power is brought over from HEMcore (rather than using a separate supply) so that both components can share the same battery back-up system.

Eight 12–48 V_{dc}, 10 A, input/output interfaces for sources and loads. Screw terminals are provided allowing for eight pairs of input and output connections (together referred to as a node). Rather than providing channels for specific purposes (sources, loads, or storage) the design decision was made to provide eight generic channels. During the development phase this will enable more flexible configuration of HEMdc, at the cost of a more complicated external wiring setup. This configuration also ensures that each channel can accommodate currents up to 10 A.

Energy metering. Each of the eight nodes has an LTC2946 energy metering IC [76]. This IC measures voltage, current, power, energy, and charge. Accuracy for all measurements is ±1%. Each IC communicates to HEMcore via the I^2C interface through a multiplexer.

Latching relays. Relays are used to connect and disconnect loads and sources at each of the eight nodes. Relays are driven by a GPIO multiplexer with an I^2C interface. Latching relays were chosen so that a loss of power or communication on HEMdc will not affect operation of user loads and sources. The status of each node is stored by the HEMapp periodically so that in the event of a loss of communication or power, the previous state of all relays can be restored immediately upon reconnection.

Full schematics for HEMdc are provided in appendix A, along with information about the Gitlab repository where the PCB design files are available.

Chapter 4

Experimental verification of HEMdc

4.1 Introduction

Microgrids are often powered by a high ratio of renewable energy resources, such as wind, water, and solar power. This is done for many reasons, including availability of such resources, cost savings from avoided fuel purchase, and reduced pollution and emissions. However, inherent in this design choice is the unpredictability, intermittency, and limited dispatch ability that comes with such resources. As a result, energy storage is often used in microgrids to supplement renewable energy resources, and ensure power availability at times when wind, water, and solar power are not available. Of energy storage resources, batteries are the most ubiquitous, and are desirable as an affordable, mature technology that can be easily scaled up or down [77].

4.2 Battery management

As an integral component of microgrids, accurate monitoring and intelligent control of the battery is required. While many manufacturers advertise useful battery lives of five years or more, achieving this lifespan requires intelligent operation and depends on number of factors, including rate of charge and discharge, ambient temperature, and depth of discharge [78, 79].

Two experiments were conducted using HEMdc to verify its ability to effectively monitor and manage batteries. The experiments focus on two aspects of battery management: first as an individual resource managed by an isolated homegrid, and second as a shared resource among the homegrids within a microgrid. Both tests rely on the ability of HEMapp to properly determine the battery state-of-charge (SOC).

4.2.1 Individual battery management

In the most basic energy storage system, the battery is connected directly to loads and supplies power until it is depleted, and remains depleted until a charging resource (such as grid connection or solar PV input) is available. This results in two problems: first, if low-priority loads are connected simultaneously with high-priority loads, the former will increase the rate of battery discharge; low priority loads will be served at the expense of more critical loads. Secondly, deep discharge of the battery will occur regularly, reducing its useful life [80].

Thus, a battery management algorithm which can prioritize loads, and prevent deep discharge of batteries, is desired. Design of such a system is described in section 4.3, and testing of the system is performed in section 4.4.

4.2.2 Collective battery management

In off-grid power systems utilizing SHS or similar technology, during times with no solar resource availability, batteries in some homes may be depleted, while those in other homes will not be. Using the MEM system, MEMcloud tracks the SOC of the batteries in each homegrid, and creates connections where appropriate to allow under-utilized storage capacity to benefit other users. In practice, such a capacity sharing system would likely be accompanied by a rate structure whereby users with excess capacity would be compensated for sharing this resource with the microgrid.

Following the design discussed in section 4.3, an experiment to demonstrate the functionality and benefit of such a system for two homegrids is described in section 4.5.

4.2.3 Hardware and software for testing

The testing rig used for all experiments described in this section is shown in fig. 4.1. Two homegrids with their own batteries and loads were connected on one cart, with a wired connection for power sharing. Homegrid 1, on the left, consists of the HEMcore board, interfaced to loads through the HEMdc board. Homegrid 2, on the right, is comprised solely of the HEMcore board, directly interfaced with dc loads. This is a previous version of the HEM hardware built prior to the development of the HEMdc interface. The loads pictured include fans and lights.

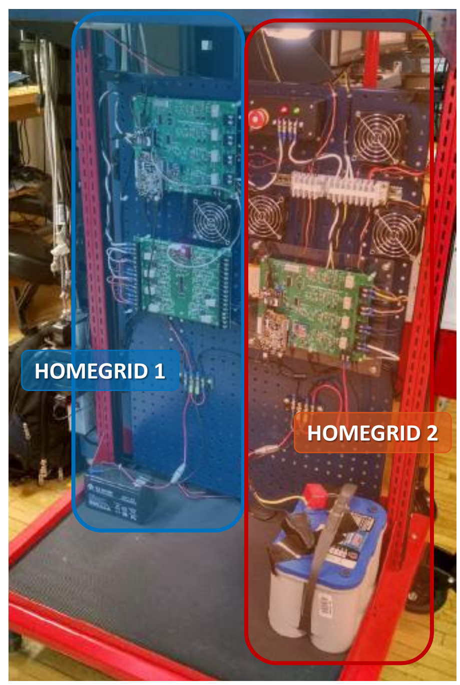

FIGURE 4.1: Test setup used for HEMdc verification experiments

Details of the C and Python code used for the experiments is provided in appendix B, along with links to the Gitlab repositories where the code is maintained.

4.3 Use of batteries in dc homegrids

4.3.1 Choice of batteries

The HEMdc system utilizes valve-regulated lead-acid (VRLA) batteries, also known as sealed lead-acid (SLA) or simply lead-acid batteries. Specifics of the two models of battery used in the experiments described in this chapter are included in table 4.1.

Make	Model	Type	V_{nom}	Capacity (Ah)	V_{empty}	V_{full}
Optima	Bluetop D34M	AGM	12	55	11.2	13.1
B.B. Battery	BP7-12	Gel	12	7	10.5	12.8

TABLE 4.1: Selected details of batteries used for HEMdc experiments

Lead-acid batteries are the most common type used when a UPS, microgrid, or back-up power system incorporates batteries for energy storage. This popularity is due to wide availability, low cost, and familiarity [81, 82]. Tubular lead-acid batteries allow for deep discharge, making them well-suited to microgrids and renewable energy technology (RET) applications [80]. The well-developed lead-acid recycling industry (able to recycle up to 95% of lead in batteries) is also a tremendous advantage, lowering cost and reducing environmental impact [83]. Development efforts specific to microgrid and related applications have focused on increasing specific energy (capacity to weight ratio, measured in Wh/kg) and deep-discharge cycle life [80].

Another battery technology, lithium-ion (Li-ion), is beginning to show promise as an energy storage means for microgrids and RETs. Since first being commercialized in the 1990s, the chief advantage of Li-ion has been its high energy density, making it ideal for mobile devices and electric vehicles, where weight and bulk are important factors [83]. But, its comparative cost has kept it out of the picture for renewables. Recently, the rapid growth in the electric vehicle market has spurred further development of Li-ion technology [84]. This increases the opportunity for the other advantages of Li-ion, chiefly its higher power rate and cycle life, to develop and outweigh its disadvantages compared to lead-acid [82]. With growing demand, improvements in materials sourcing and recycling are also likely.

4.3.2 Calculating state-of-charge

The first step in managing batteries is accurately monitoring the level of charge. HEMdc interfaces with its power source(s) directly through the battery, counting the flow of charge from the battery to the loads by direct measurement using an energy monitoring IC at each load–the LTC2946 [76]. The IC measures charge (in coulombs, C) with an accuracy of $\pm 0.6\%$. By counting the coulombs flowing to each load, and knowing the total capacity of the battery, HEMapp can determine the change in SOC.

The initial SOC (a value between 0 and 1) is calculated based on the open circuit voltage $V_{oc}(t_0)$ measured each time HEMapp begins running, assuming that the battery has been in an open-circuit state for some time [85–87]:

$$SOC(t_0) = \frac{V_{oc}(t_0) - V_{empty}}{V_{full} - V_{empty}} \tag{4.1}$$

Values for V_{full} and V_{empty} are provided by the battery manufacturer, and represent the expected equilibrium open circuit voltages when the battery is fully charged and depleted, respectively.

The assumption that the battery has been left in an open circuit state for some time is critical, as several hours may be required for lead-acid batteries to reach equilibrium after charging or discharging [86].

With the starting value for SOC known, the change can be calculated from subsequent measurements in the charge, Q:

$$\Delta SOC = \frac{Q[\mathbf{k}] - Q[\mathbf{k}-1]}{Q_c \times 3600} \tag{4.2}$$

The LTC2946 provides an accumulating register recording coulombs flowing from a source to a load. This value, Q, is updated by the IC every 16 ms (based on an external oscillator), and read by HEMapp approximately every 5 s (denoted $Q[\mathbf{k}]$ to indicate the discrete nature of the measurement). The factor of $1/3600$ is used to convert between Ah (the unit of measure of battery capacity) and C.

Finally, the value of SOC is updated continuously by HEMapp by subtracting ΔSOC each time it is calculated.

4.3.3 Charge management algorithm

HEMapp uses SOC to make decisions about when to allow power export, request power import, and enable or disable loads. Each of these actions enables HEMapp to meet its four objectives, in order:

1. Prevent over-discharge of battery
2. Reserve sufficient battery charge to serve high priority loads
3. Provide power to lower priority loads as often as possible
4. Export power to other homegrids to sustain the larger microgrid

Various thresholds are set within the HEMapp to make decisions and accomplish these goals. The general process is shown in the flowchart of fig. 4.2. For each threshold that is set, different actions are defined.

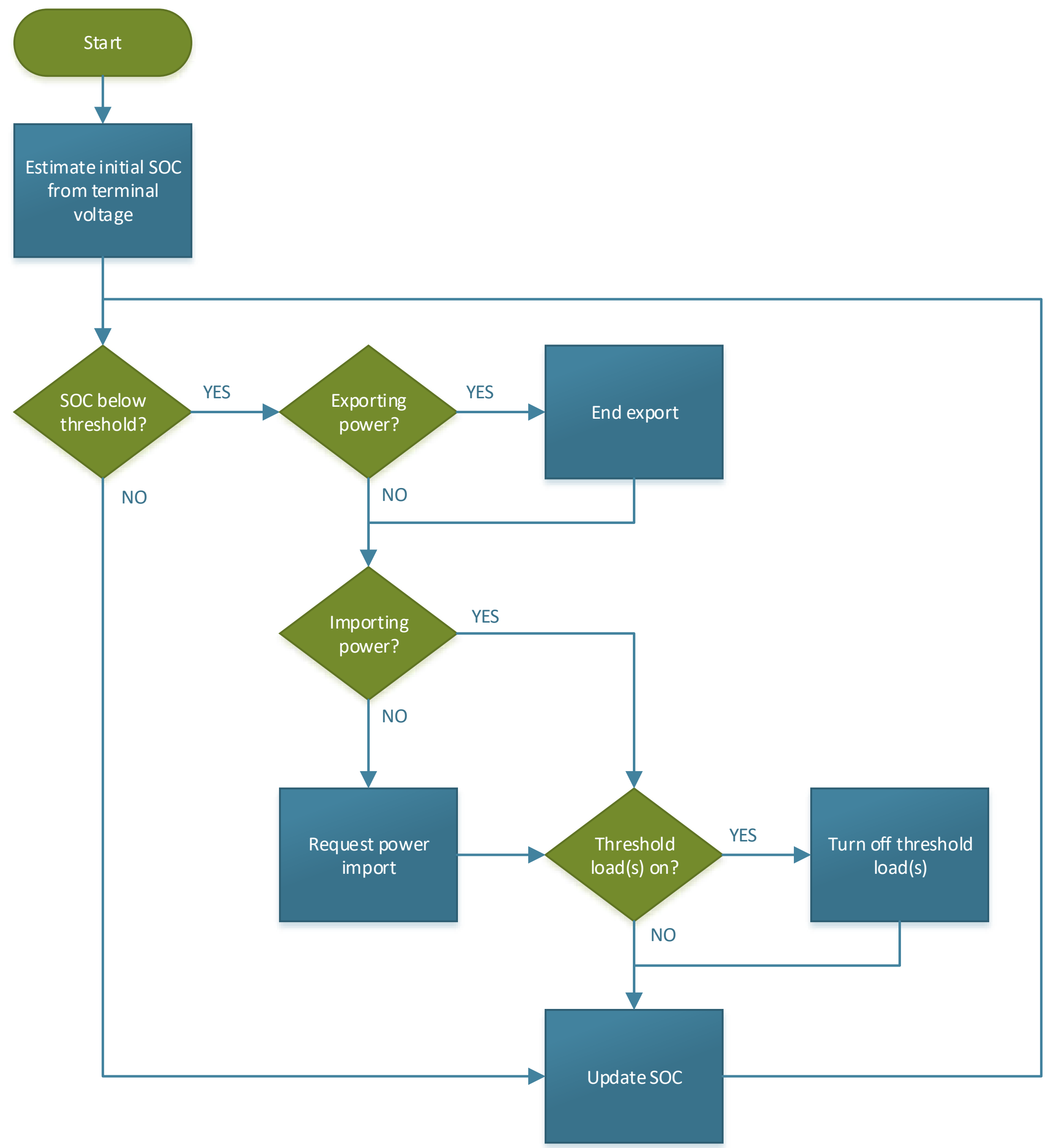

FIGURE 4.2: Flowchart describing HEMapp decisions based on battery SOC

4.4 Individual battery management experiment

To test the basic functionality of SOC calculation and the ability of HEMapp to use this information, the following test was established. A HEMdc system was connected with three loads of different priority levels:

High priority: 0.5 W LED light; powered when SOC exceeds 25%

Medium priority: 3 W LED light; powered when SOC exceeds 50%

Low priority: 7 W cooling fan; powered when SOC exceeds 75%

The system was connected to the 7 Ah battery of table 4.1. With a fully charged battery, HEMapp was started, and all three loads were powered on. The test was run twice for 14 hours, with and without the battery management algorithm in place. As the battery was depleted past the thresholds at 25%, 50%, and 75%, loads were disabled starting from the lowest priority.

4.4.1 Results and discussion

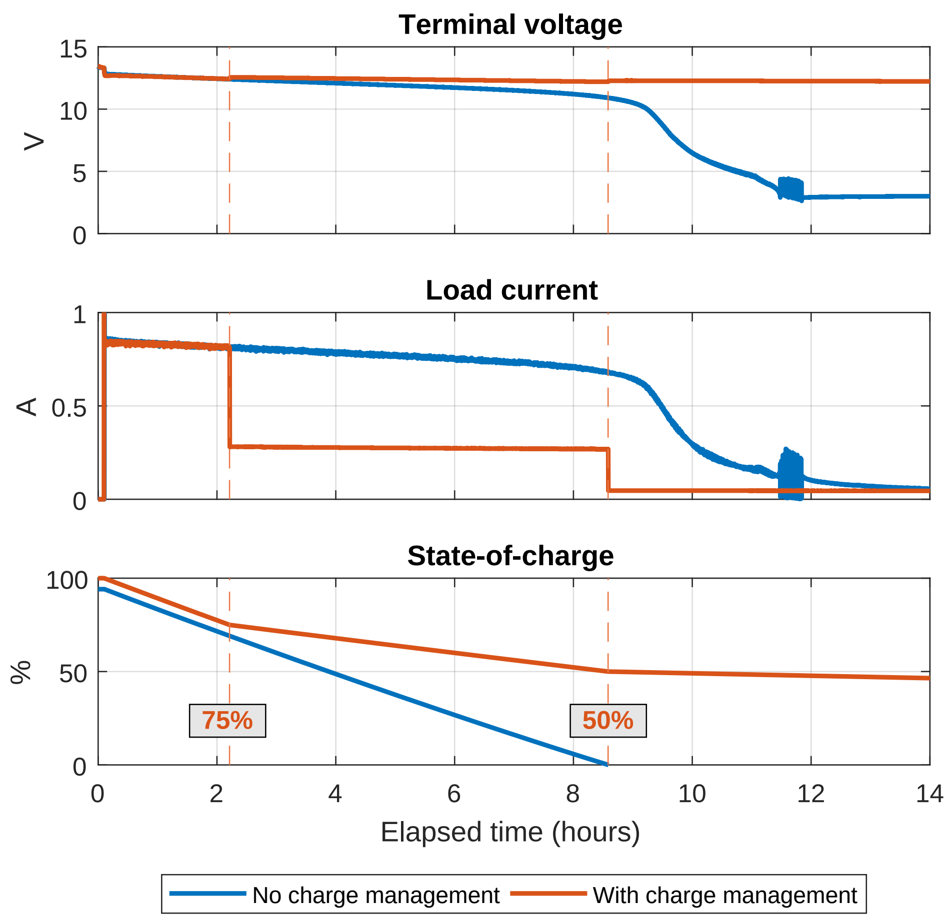

FIGURE 4.3: Waveforms of battery voltage, load current, and battery SOC, illustrating operation of HEM with load switching during different states

Results are shown in fig. 4.3. In the scenario with no battery management (blue line), no loads are being served at all after 12 hours, and in the interval from 9 to 12 hours, current to the loads diminishes rapidly, resulting in the erratic usage shown just before the 12th hour. In a real-world scenario such erratic behavior could result in damage to the loads, battery, management equipment, or all three.

In contrast, with the management algorithm running (red line), the high priority load is served for the duration of the test, and the medium priority load (powered off when

SOC reaches 75%) is served for approximately the same duration as it had been in the test with no battery management. The low priority load (which had the highest usage in this scenario) is served for just over two hours. At the end of the test the battery retains nearly 50% charge.

4.4.2 Future improvements

In a real-world scenario, the priority of loads would be determined by the user through a simple ranking mechanism. Setting specific values for the SOC thresholds is an area of on-going research. Current development of the HEM system involves automatic calculation of the thresholds by the HEMapp based on the quantity and size of the loads, and other factors such as battery capacity, type, and age. Longer-term work proposes varying the thresholds based on time of day (a predictor for solar energy input), availability of power export from neighboring homegrids, and occupancy (whether the homegrid users are present or not).

Additionally, factors such as self-discharge and ambient temperature will need to be included in the real-time calculation of SOC in order to improve accuracy, especially over the lifetime of a battery.

4.5 Collective battery management experiment

A second experiment was conducted to test the ability of two homegrids to manage battery capacity collectively. As described in fig. 4.2, as SOC reaches specific thresholds, HEMapp makes decisions about starting or stopping power import or export. The various thresholds programmed for each homegrid for the power sharing tests are described in table 4.2. This table also gives the nominal power rating of the two loads (high priority and low priority) for each homegrid.

Threshold	Action
60%	Disable power export
50%	Request power import
40%	Disable low priority load **(4.5 W)**
10%	Disable high priority load **(5.5 W)**

TABLE 4.2: Threshold definitions and actions for the two homegrids of the power sharing test

To demonstrate the advantage of power sharing, the two homegrids used batteries of different total capacity of the test. Details of the batteries and their SOCs at the beginning and end of each test (base case and actual) are given in table 4.3.

Homegrid 1 ❘ *7 Ah battery*		
	Initial SOC	**Final SOC**
Base case	98%	10%
Test case	94%	16%
Homegrid 2 ❘ *55 Ah battery*		
	Initial SOC	**Final SOC**
Base case	84%	60%
Test case	86%	54%

TABLE 4.3: Details of homegrid batteries and SOCs for power sharing test

4.5.1 Baseline

A baseline was established by charging both batteries and running both homegrids without the ability to share power. During the 14 hours of the test, no external power source was used to charge the batteries, and no loads were toggled manually. HEMapp executed load curtailment as needed based on SOC. Results for this scenario are shown in fig. 4.4.

In this scenario, homegrid 2 maintains sufficient charge to avoid the need for load curtailment, while homegrid 1 passes two thresholds, requiring it to curtail all loads after roughly 9.5 hours.

4.5.2 Power sharing enabled

Next, power sharing was enabled in the HEMapp algorithm. As in the base case, the test started with all loads switched on, and batteries fully charged. The power sharing link was initially disconnected.

Request for power export is accomplished automatically, with the "importing" homegrid sending an SMS to the "exporting" homegrid. The exporting homegrid initiates the export as long as its own SOC is above the programmed threshold.

When power export is active, the local battery for the importing homegrid is left active–this is to ensure that local loads will continue to be served in the event that the exporting homegrid ceases exporting, or if there is a fault on the power lines linking the two homegrids.

4.5.3 Results and discussion

Plots of terminal voltage, current, and SOC are shown in fig. 4.5 for the duration of the test.

From the plots it can be seen that when the SOC for homegrid 1 reaches 50%, it requests power export from homegrid 2. Homegrid 2 initiates the export (indicated by

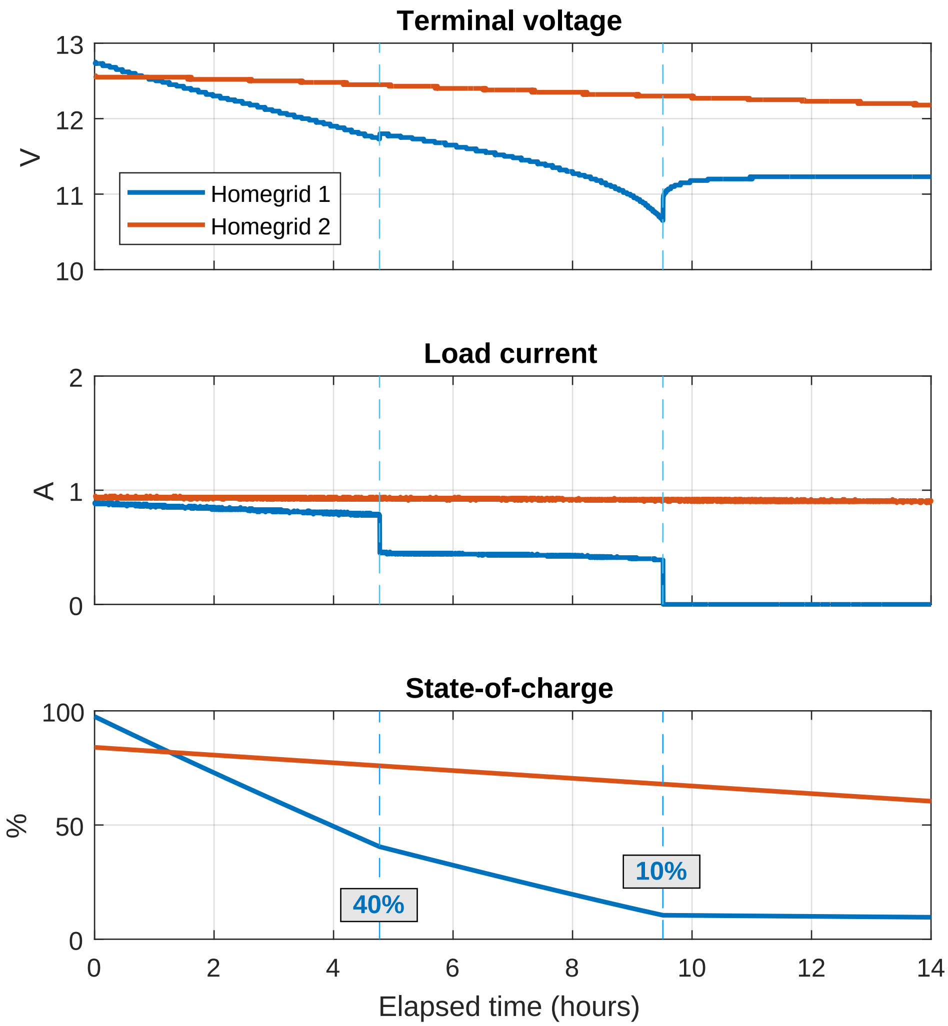

FIGURE 4.4: Waveforms of battery terminal voltage, load current, and battery SOC, illustrating **base case** of two homegrids with power sharing disabled

the purple shaded region) until its own SOC diminishes below 60%. Shortly after this, homegrid 1 reaches 40% and curtails its low priority load.

After 14 hours the test ends. At this point, homegrid 2 still has both of its loads enabled (as in the base case), while homegrid 1 still has its high priority load enabled– unlike the base case, where all loads were curtailed after 9.5 hours.

Additional detail for the time period during which power sharing is active is given in fig. 4.6.

An interesting result can be observed for the first several minutes after power sharing is enabled. The start of power sharing equates to directly connecting the two batteries of each homegrid. This causes a period of instability in the system, where the voltages of the two homegrids fluctuate. As a result, the share of power supplied to the loads at the importing homegrid fluctuates between the remote and local batteries for several

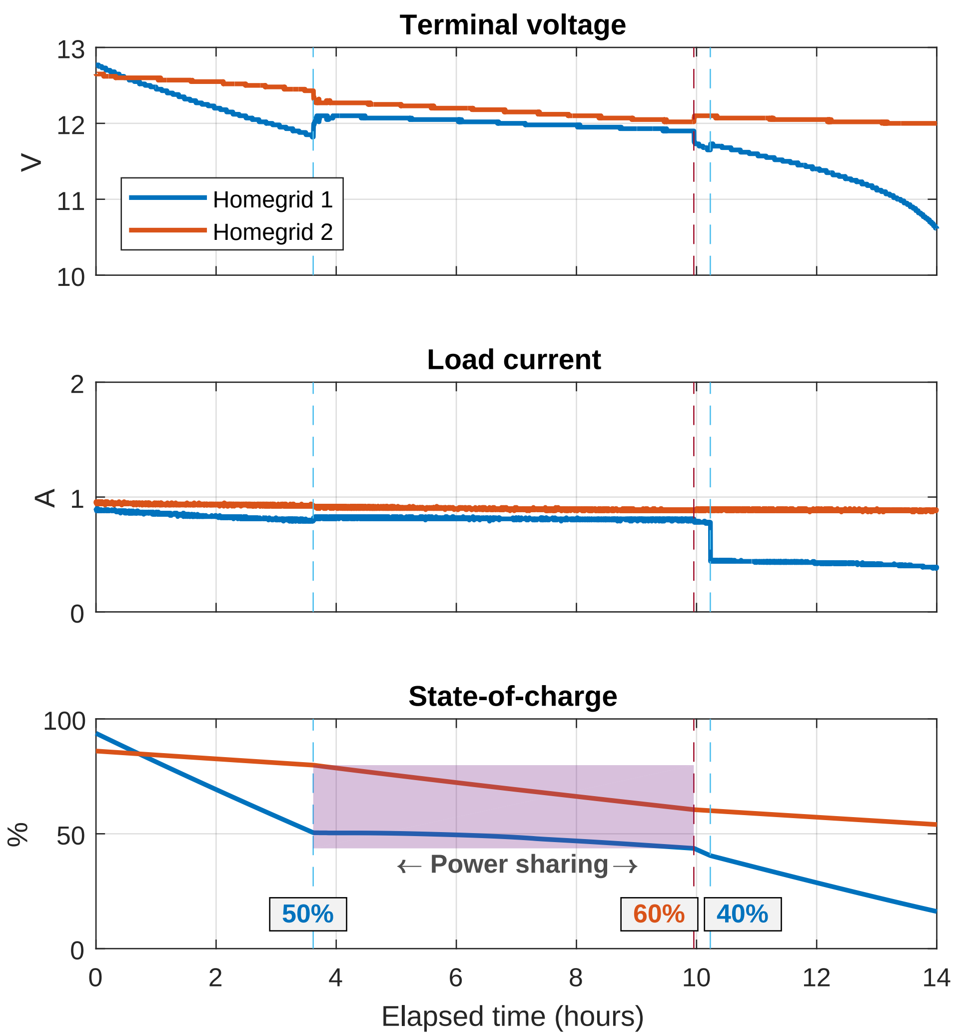

FIGURE 4.5: Waveforms of battery voltage, load current, and battery SOC, illustrating operation of two homegrids with **power sharing enabled** (see description of thresholds in table 4.2)

minutes.

Just after the seven hour mark, another destabilization event nearly occurs, with the current drawn from the battery at homegrid 1 beginning to rise sharply. More work is needed to study and prevent these types of events when power sharing between two homegrids is enabled.

4.6 Conclusions and future work

The tests performed in this section demonstrate that the HEMapp is able to intelligently manage a homegrid's battery by measuring SOC, and using this data to curtail loads

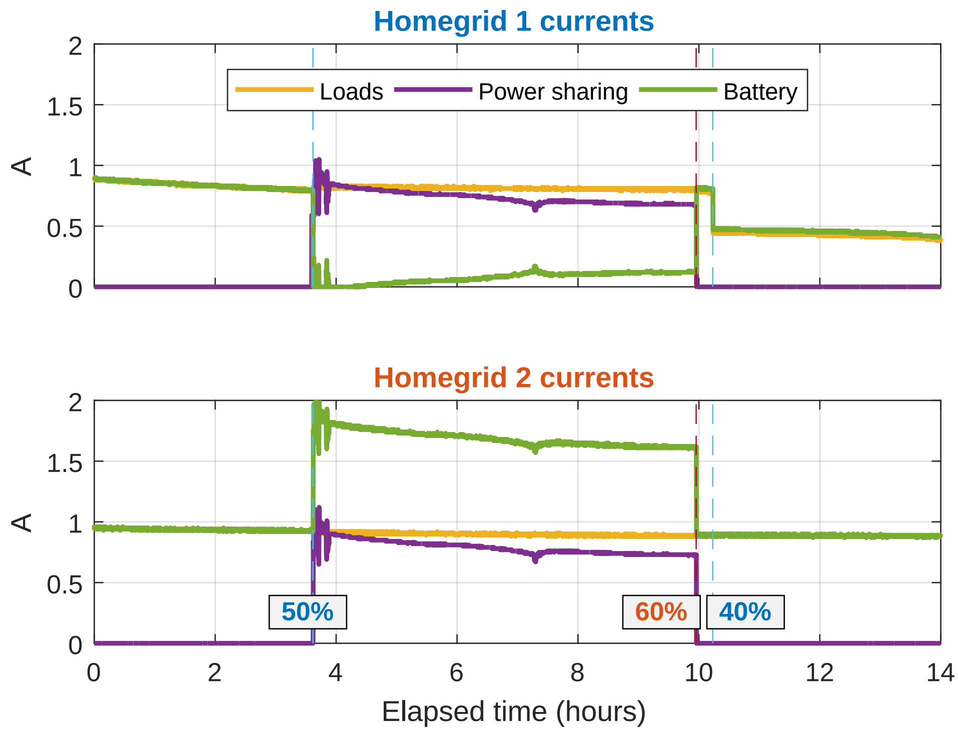

FIGURE 4.6: Current waveforms for two homegrids with power sharing enabled (to keep plot scales consistent, "Power sharing" is represented as a source in Homegrid 1, and a load in Homegrid 2)

based on priority. Additionally, when two homegrids are connected, HEMapp is able to manage sharing of power between them to further prolong battery life.

In a real-world situation, HEMapp would require additional information to properly prioritize between powering local loads, and sharing power with other homegrids. For instance, there may be scenarios where a local load could be curtailed to continue supplying power to a remote load. This could represent a situation where the potential income from selling excess power is deemed more profitable than some local use of power. The opposite scenario could also be true–rather than requesting power import, HEMapp may choose to curtail a local load if such a decision is deemed to be less costly.

Chapter 5

Microgrid work at NIE-CREST

5.1 Introduction

From February to May of 2015 Professor Giri Venkataramanan completed a teaching sabbatical at the National Institute of Engineering (NIE) in Mysuru, India [88]. While working with a group of students on construction of a microhydro generator (see section 5.4.1.2), he forged a relationship with Professor Shamsundar Subbarao, Associate Professor of Mechanical Engineering at NIE, and director of CREST, the Centre for Renewable Energy and Sustainable Technologies. The two proposed a partnership between their two institutions to cooperate on microgrid research, development, and testing. Professor Giri's research group would provide research expertise and system design, while CREST would provide space for testing, project management for implementation, and expertise on biofuels.

Project collaboration began in December 2015 when Professor Giri and two students (including the author) traveled to Mysuru for three weeks to set up small-scale microgrid test-bench and run a workshop on microgrids with a group of NIE undergraduate students from various engineering disciplines.

In May 2016, the two institutions signed a memorandum of understanding, "to promote academic cooperation [...] with a focus on expanding scholarly ties and exploring the feasibility of establishing a framework for educational and scientific cooperation" [89].

To date, the author has traveled three times to CREST to collaborate on microgrid research and development. Other members of the microgrid project team from UW-Madison are scheduled to travel to NIE in summer 2017 to continue working on the project.

In the following sections a brief outline of each visit is given, followed by documentation of the work completed, and specifications of the systems currently in place at CREST.

5.2 Summary of work

Dates of the three visits completed to date are given below, followed by a brief description of the goals and outcomes from each visit.

Phase 1 (December 2015 to January 2016): Install and test energy sources (wind, hydro, solar, and biodiesel) and connect to dc microgrid testbeds

Phase 2 (June to August 2016): Upgrade microgrid control hardware, integrate live office loads (interior and street lighting), set up biodiesel generator remote start system

Phase 3 (April 2017): Implement prioritization and scheduling of live loads, interface with 10kW library solar system, improve control of streetlights

5.2.1 Phase 1 – December 2015 to January 2016

Professor Giri, the author, and fellow graduate student Ashray Manur traveled to NIE for three weeks in December 2015 and January 2016. During this initial visit, the team worked with a group of about 20 undergraduate students in various engineering disciplines, including electrical, electronics, and mechanical.

The primary goal of the workshop was the implementation of four isolated microgrid testbeds incorporating various combinations of energy sources, storage, and both ac and dc loads. To this end, work on four separate energy sources was completed: solar arrays, a wind turbine, a microhydro, and a bio-diesel generator.

In addition, two separate systems for microgrid monitoring and control were tested and implemented: one for ac loads which relied on wifi and wireless mesh for communication, and one for dc loads with a GSM modem for communication by text message (SMS). Elements of both systems were later combined into the MEM platform discussed in chapter 3. A number of design and technical issues with the two systems meant that their functionality was limited, but the work done was important for laying the groundwork for later progress.

5.2.2 Phase 2 – June to August 2016

Over the summer of 2016 the author traveled to Mysuru alone to work with a group of approximately 30 students, including several from the earlier group.

Students were organized into groups of four to six, each working on one aspect of the microgrid system. Work done included adding additional solar panels, performing a load study of the CREST office, producing as-built wiring diagrams, and automating control of the bio-diesel generator.

Phase 1 team at NIE (photo by CREST staff, 2015-12-29)

Phase 2 team on a trek to Bettadapura (photo by author, 2016-07-07)

FIGURE 5.1: Team photos from phases 1 and 2

During this phase, the control hardware was upgraded to a more powerful dc-only system, which integrated control, communication, and monitoring aspects of both the ac and dc hardware used in phase one.

In addition, the students visited two tribal hamlets to determine suitability for future electrification projects (see section 5.6).

5.2.3 Phase 3 – April 2017

The purpose of the author's final visit to Mysuru was supporting four groups of students completing their final year projects, each incorporating some aspect of the microgrid:

Library interconnection. Study of the 10 kW solar power system at the library, and connection of an ac line from the library to CREST to allow excess power to serve as an alternate source for the CREST microgrid.

Load prioritization algorithm. Development of an algorithm on the existing dc microgrid hardware to enable or disable loads based on priority and battery charge level.

Streetlight automation. Load study and automation of four streetlights outside CREST office, including scheduling around dusk and dawn, and increasing brightness when cars and pedestrians approach.

Vertical-axis wind turbine. Testing and characterization of a custom-made vertical-axis wind turbine using an off-the-shelf permanent magnet dc machine.

A site visit to another potential site for microgrid implementation was also conducted.

5.3 CREST description and setting

CREST is located in the city of Mysuru, in the state of Karnataka in southern India. The main campus is at N12°16.8′ E76°38.5′. A satellite image of the main NIE campus, showing the location of the various CREST microgrid elements, is given in fig. 5.2. The map was created in Google My Maps and can be viewed interactively on-line at: `https://goo.gl/YG3JKN`. Additional images are included in the on-line version, as well as a scale for estimating distances. Selected annual average weather data for the city of Mysuru is given in fig. 5.3.

FIGURE 5.2: Satellite image of NIE campus indicating location of CREST microgrid elements. View on-line: `https://goo.gl/YG3JKN`. Map data: Google Imagery, CNES / Astrium, DigitalGlobe (2017).

CREST is run by a staff of five full-time employees. The office is intended to support typical tasks such as hosting meetings, using computers, filing documents, and storing project materials. For educational purposes, there is a small library and a full-size classroom with projector and sound system. In addition, the office includes a bathroom and small kitchen.

The office occupies roughly 200 m^2 on the top floor of a two-story concrete building. The main office space has windows facing north and west; the kitchen and bathroom

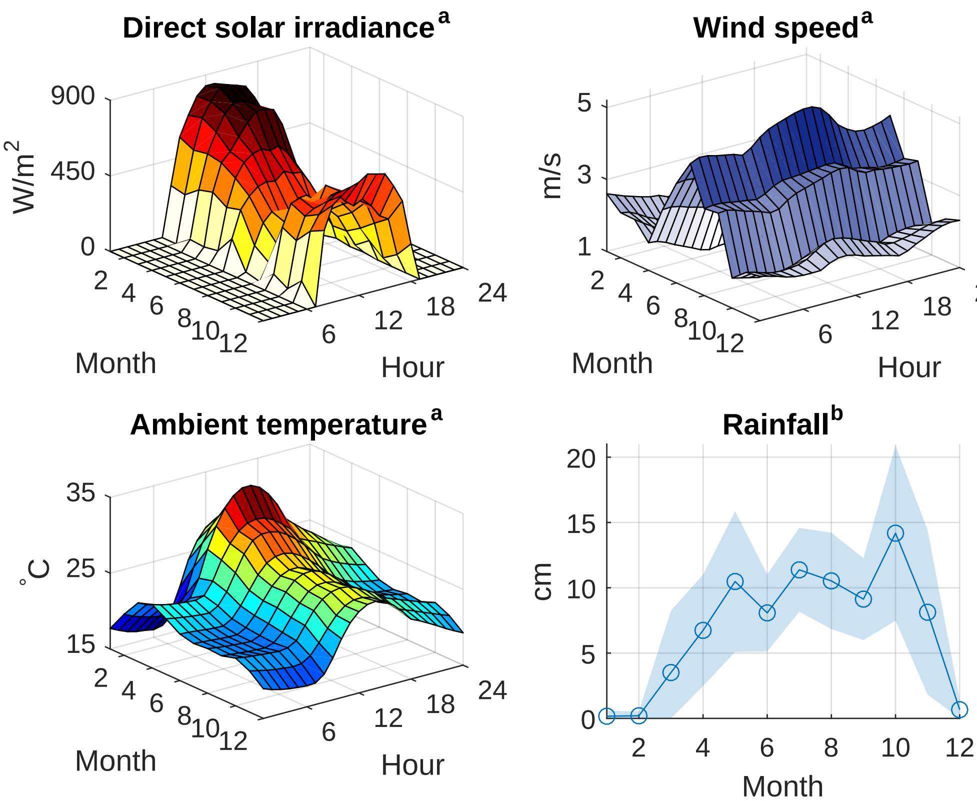

^a Hourly solar, wind, and temperature from satellite-derived 10km grid data, averaged over 2002 to 2011 [90]

^b Average monthly rain data for Karnataka state, measured by rainguage, averaged over 2004 to 2010 [91]. Bounded line shows one standard deviation.

FIGURE 5.3: Selected annual weather data for Mysuru

line the eastward facing wall. The roof above is flat, and accessible only by ladder from the outside of the building.

5.3.1 CREST office wiring and loads

Power comes into the office at one location, where it branches in two: one line supplying secondary lighting and ceiling fans, and the other diverted through an uninterruptible power supply (UPS). From the UPS, one line supplies computers, a projector, and plug loads (mainly fans), while a second line supplies primary lighting. At peak, the UPS supplies 1000 W for lighting and computers (including 600 W for the projector). The non-UPS load is 750 W peak. Loads and other details of the UPS are included in table 5.5 along with details on the microgrid testbeds.

Appendix C contains additional details of the office wiring: A simplified one-line diagram is shown in fig. C.1, and the office electrical layout is given in fig. C.2.

5.3.2 CREST office networking

The CREST office has a dedicated Wi-Fi network (independent from the NIE Wi-Fi network), and a LAN network switch. The general settings to be used for any device on the LAN are given in table 5.1. For a specific IP address and network access it is necessary to communicate with the NIE network administrator.

IP address start	192.168. 19. 2
IP address end	192.168. 19.253
Gateway	192.168. 19. 1
Subnet mask	255.255.255. 0
DNS	118.151.209. 5
	118.151.209. 6

TABLE 5.1: CREST LAN details

5.3.3 NIE library solar power system

Professor Shamsundar was instrumental in obtaining and installing a solar power system for the NIE College library. The system consists of seven strings of the same a-Si panels in use at CREST (see table 5.2), for a total of 8,600 kW. Energy storage consists of 15 tubular lead-acid batteries with 210 Ah capacity each, for a total capacity of 3,150 Ah. A power conditioning unit, including MPPT charger and inverter, manages battery charging and source selection between solar, battery, and mains back-up.

During phase three, as a student project, a wired ac connection was installed between the library and CREST, to allow excess power from the library solar system to be exported to CREST. Automation of the power export requires accessing the real-time data which is stored on the PCU. The NIE students attempted to access this data using a Beaglebone Black (BBB) single-board Linux computer (which also serves as the core of the MEM system). Unfortunately, it was determined that the serial-to-USB port installed on the PCU is not compatible with BBB. Real-time data export from the PCU was successfully demonstrated, but could not be maintained consistently. At the time of writing, the students were in communication with the PCU vendor to resolve this issue.

5.4 Systems in place at CREST

5.4.1 Energy sources

Four principal energy sources are established at CREST: solar, wind, hydro, and bio-diesel. Specifics of each energy source are given below. The locations described refer to the layout given in fig. 5.2.

5.4.1.1 Solar panels

Two different solar panel technologies are in use in the microgrid system at CREST: amorphous silicon (a-Si), and multicrystalline silicon (multi-Si, also called polycrystalline silicon or polysilicon). The types and quantities of each panel in use as of this writing are shown in table 5.2.

Type	Quantity	V_{nom}	V_{OC}	I_{SC}	P_{max}	V_{MP}	I_{MP}	Make	Model
multi-Si	2	12	21.0	2.400	35	16.2	2.200	Ammini	ASM-12035A
multi-Si	2	12	21.4	3.150	75	17.7	4.250	Su-Kam	POLY 12-075
multi-Si	2	24	43.2	4.650	150	34.1	4.400	Su-Kam	POLY 24-150
a-Si	28	48	101.0	0.787	43	71.0	0.616	Solarex	MST-43MV

TABLE 5.2: Selected details of solar panels at CREST (values for dc) [92, 93]

The multi-Si panels in use were either purchased by or donated new to CREST. The a-Si panels were obtained free of charge when they were removed from a local installation that was upgrading to newer, more efficient panels. (The manufacturer of the a-Si panels, Solarex, was acquired by BP Solar in 1999; in 2010 BP Solar shut down the Solarex production facilities, and in 2011 BP Solar was dissolved [94, 95].)

This type of panel was once very popular, however two key disadvantages have reduced its popularity over time. First, despite making rapid advances in efficiency in the early years of development, over the last several years the peak efficiency of a-Si cells has stabilized at 10 to 14%, well below that of crystalline silicon technologies, which range from 21.2% to 27.6% [96–98].

Second, degradation rates of a-Si are noticeably higher than those for multi-Si [96]: a literature review of studies of real-world installations found that post-2000, a-Si systems had a median degradation rate of 0.87% per year per module, compared to 0.64% for multi-Si [99].

The a-Si panels and two of the multi-Si panels are located on the roof of the building adjacent to CREST (see photo, fig. 5.4a), with the balance of the multi-Si panels on the roof of CREST itself.

5.4.1.2 Microhydro

The custom-built microhydro generator which Professor Giri had worked on previously is located in the fluid mechanics lab; fig. 5.4b shows it in operation.

The machine used in the microhydro is a standard automotive alternator. To operate, a battery must be connected to excite the alternator; this battery also serves to store the energy produced once it is running. To export power to the microgrid, a 200 W inverter is connected to the battery to produce 220 V_{ac} power for transmission (by a line run to the CREST office which also carries power from the genset).

(A) The a-Si solar panels (photo by author, 2016-01-01)

(B) The microhydro generator in operation (photo by author, 2015-12-29)

FIGURE 5.4: Solar and hydro energy sources for CREST microgrid

At the time of writing the microhydro was undergoing modifications and improvements, including addition of an enclosure to improve water flow.

5.4.1.3 Wind turbine

A 400 W Air X wind turbine from Primus Wind Power was pole-mounted on the roof of the CREST building and wired into the office (selected details in table 5.3a). At the time of writing the staff at CREST were awaiting a shipment of replacement parts (yaw assembly and governor) to repair damage to the turbine caused by improper assembly during phase one.

In addition, during phase three a student group built and began testing of a vertical axis wind turbine (see fig. 5.5a). The turbine uses an off-the-shelf 300 W, 12 V_{dc} permanent magnet motor. At the time of writing, the students were testing the turbine at various speeds using a large fan to characterize its performance.

(A) Vertical-axis wind turbine (photo by author, 2017-04-15)

(B) Bio-diesel generator (photo by author, 2016-07-05)

FIGURE 5.5: Wind and bio-diesel energy sources at CREST

5.4.1.4 Diesel generator

A 3 kVA diesel generator, model CC1-3AS [100] was purchased and located in an open-air lab, connected to the CREST office by a 220 V_{ac} line (which also carries power from the microhydro). The generator is run using a mixture of 80% diesel and 20% bio-diesel, the latter produced at CREST. Selected details are given in table 5.3b.

(A) **Wind turbine**

Wind speed details	
Startup	3.6 $m\,s^{-1}$
Operating range	3.6 – 22 $m\,s^{-1}$
Optimum range	11 – 15 $m\,s^{-1}$
Rated power output	12.5 $m\,s^{-1}$
Maximum	49 $m\,s^{-1}$
Electrical characteristics	
Machine type	Permanent magnet
Rated power	400 W
Nominal voltage	12 V_{dc}
Output voltage	14.1 V_{dc}
Physical characteristics	
Swept area	1.07 m^2
Rotor diameter	1.17 m
Weight	5.9 kg

(B) **Genset**

Generator	
Power at rated speed	3 kVA
Voltage	230 V_{ac}
Frequency	50 Hz
Power Factor	0.8
Engine	
Rated output	3.38 kW / 4.6 hp
Cylinders	1
Displacement	306 cm^3
Rated speed	3,000 rpm
Performance at rated power	
Alternator efficiency	74%
Voltage dip	<20%
Time to rated output	<5 s
Fuel consumption	1 $L\,h^{-1}$

TABLE 5.3: Selected details of **(A)** the wind turbine [101]; and **(B)** the bio-diesel genset [100] at CREST

Remote start of generator. The generator includes an ATS interface with a 5-pin, 240° DIN 45322 connector. The pins are:

- Battery positive
- Battery negative
- Generator contactor relay
- Mains contactor relay
- Auto start switch

By connecting auto start switch to battery negative, the generator can be started. The generator and mains contactor relays are used to control which source is supplying power to the load–for the application at CREST, these connections are not needed, as the generator is only run to supply back-up power when called for by the MEM cloud application (see chapter 3 for further details).

Under normal operation, a trickle-charge voltage of 13.8 V_{dc} should be supplied for battery maintenance.

During phase 2 of the project, a successful test of a remote generator start system was conducted. The phase 1 control hardware, no longer in use in the microgrid test-beds, was programmed and wired to start the generator using a relay when a text message containing the words "GENERATOR ON" was received. Sending "GENERATOR OFF" opens the relay, shutting off the generator. The internal controller for the generator delays starting and stopping as necessary to ensure proper warm-up and cool-down times.

5.4.2 Power conversion

Two key power conversion systems are in place at CREST: battery chargers, and ac inverters.

5.4.2.1 MPPT chargers

The batteries (section 5.4.3) for each microgrid testbed are charged from the solar PV panels using battery chargers with Maximum Power Point Tracking (MPPT). Solar PV cells exhibit a non-linear V-I curve, varying with ambient temperature and solar irradiation–see fig. 5.6 for an example. A given point along this curve will be the maximum power point, where the panel will produce the maximum possible power output for a given temperature and irradiation level. This point can be determined partly through calculation and partly through trial and error (or "perturb and observe"); an MPPT charger uses an algorithm intended to determine and maintain the maximum power point [102, 103].

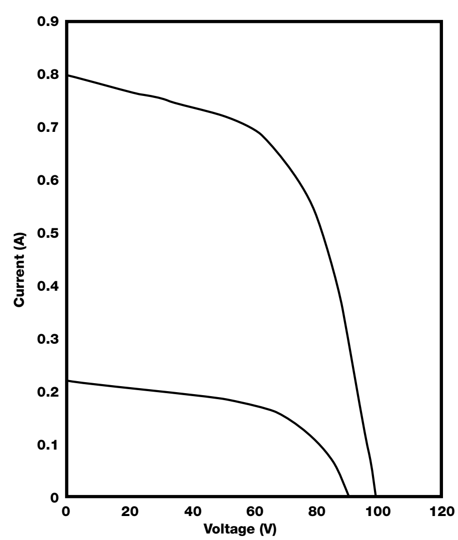

FIGURE 5.6: V-I curve for a solar PV panel [92]

Details of the MPPT chargers at CREST are given in table 5.4.

PV voltage range	17–95 V_{dc}	**Float charge**	13.8 V_{dc}
Max PV input power	450 W	**Main charge**	14.4 V_{dc}
Nominal voltage	12 V_{dc}	**Boost charge activation**	12.3 V_{dc}
Nominal charge current	30 A_{dc}	**Equalization activation**	12.1 V_{dc}
Max battery charge current	33 A_{dc}	**Equalization charge**	14.8 V_{dc}
Max efficiency	98%	**Temperature range**	-40 to +50 °C

TABLE 5.4: Selected details of Phocos 100/30 MPPT charger [104]

5.4.2.2 Inverters

Inverters are used to take power from batteries at 12 V_{dc} and convert it to 230 V 50 Hz. Two different types of inverters are in use at CREST:

UPS inverters use mains power to charge a battery bank, and supply ac loads with power from the batteries when mains power is not available. Three 700 VA UPS inverters are in use at CREST.

Solar UPS inverters use solar PV input to charge the batteries and supply loads, when available, and fall back to mains otherwise. One 2400 VA solar UPS inverter is in use at CREST.

5.4.3 Energy storage

The batteries used for energy storage at CREST are exclusively tubular lead-acid batteries. At this time, Li-ion batteries are not being used as a part of the work on MEM, but an Indian startup based in New Delhi is considering working with NIE to provide Li-ion batteries for testing, which would be done with the system in the CREST office. See section 4.3.1 for a comparison of lead-acid and Li-ion battery chemistries.

At the time of writing, eight different batteries with capacity ranging from 40 to 210 Ah are in use at CREST. Total combined capacity of all batteries is 840 Ah.

5.5 Microgrid testbeds

During the course of the three visits to CREST, four microgrid "testbeds" were established. Each consisted of a solar power source and a mix of ac and dc loads, with appropriate chargers and inverters. Selected details of the components used in each testbed are given in table 5.5. (The table also includes details for the two main circuits in the CREST office–one connected via UPS, and the other on a direct connection to mains power.)

The testbeds were color-coded for differentiation: green, yellow, blue, and red. The green testbed also includes the capability to accept wind and hydro power, though both sources were undergoing repairs and improvements at the time of writing. Schematics for all four testbeds are given in appendix C, in figs. C.3 to C.6.

The inverters for all four testbeds were connected to a single back-up line, which could be switched between mains power, and input from the bio-diesel genset. During phase 3, work began to interconnect the 10 kW solar power system at the library to the CREST office for the purpose of testing power sharing: the 220 V_{ac} line used for this purpose will also be connected to the change-over switch for selecting back-up source for the inverters. At a later date, when the HEM ac interface is completed and deployed, selection of back-up source will be automated.

	Solar input			Battery capacity (Ah)	Inverter capacity (VA)	Loads		
	Panel type	Power (W)	V_{nom} (V_{dc})			Type	Peak[a] (W)	Voltage
				Microgrid testbeds				
Green[b]	a-Si	301	48	100	700	Demo lights	15	12 V_{dc}
Blue	multi-Si	300	48	40	700	Office lights	50	12 V_{dc}
						Office lights	100	230 V_{ac}
Yellow	a-Si	301	48	40	700	Demo lights	15	12 V_{dc}
						Office lights	200	230 V_{ac}
Red	multi-Si	220	24	210	1,100	Street lights	150	230 V_{ac}
				CREST office				
UPS	a-Si	602	48	450	2,400	Lights, office equipment	1,000	230 V_{ac}
Mains						Lights, fans	750	230 V_{ac}
				Totals				
		1,724	—	840	5,600		80	12 V_{dc}
							2,200	230 V_{ac}

[a] Estimated based on quantity and type of light bulbs, fans, and office equipment
[b] The "green" testbed is also wired to accept wind and hydro as power sources

TABLE 5.5: Summary details of the four microgrid testbeds at CREST (see appendix C for schematics)

The existing control hardware for the testbeds at CREST is only capable of monitoring and controlling dc loads. It is furthermore limited to 4.5 A on any one of the four available load circuits, or a total of 8 A for the entire board. Two versions of the control hardware are shown in fig. 5.7.

(A) Hardware used during phase 1 (photo by author, 2016-01-16)

(B) Hardware used during phases 2 and 3 (photo by author, 2016-08-01)

FIGURE 5.7: Two generations of the dc load monitoring and control hardware for the microgrid testbeds at CREST

5.6 Microgrid candidate site visits

During each phase of the project, the author visited several villages which are being considered as candidates for installation of microgrids for village electrification.

5.6.1 Tribal hamlets in protected forest areas of Karnataka

During the first two visits, the author visited *hadis* (hamlets) located on protected forest lands, populated by indigenous forest dwellers (or tribal people). While a 1990 bill had guaranteed forest dwellers the right to their historical homelands, the failure of states to implement the guidelines, and a Supreme Court decision affecting the definition and jurisdiction of "forests," resulted in large-scale evictions of tribal peoples by the forest departments of various states [105–107].

Mass protests followed, putting pressure on government to act. While the federal Ministry of Forests and Environment and the Supreme Court made additional attempts to rectify the situation, nothing changed significantly until 2006, with the passage by parliament of the "Scheduled Tribes and Other Traditional Forest Dwellers (Recognition of Forest Rights) Act." The act provides a means to clearly define the boundaries of the forests and protected areas, and sets out the rights of tribal people living in those areas. At the same time, it prohibits them from certain activities, such as hunting and trapping, or large-scale cultivation [108].

An additional provision within the act calls for the government to provide for necessities such as schools, hospitals, electricity, roads, and water supply–with the stipulation that such provision cannot violate previously enacted legislation governing the types of material and construction allowed within the forests. As a result, state governments began seeking alternative means to provide necessities to the estimated 84 million forest dwellers [105].

Shamsundar (center) and Balachandran (right) address a group of NIE students

Front view

FIGURE 5.8: A bamboo anganwadi in a tribal hadi near Muthur village (photos by author, 2016-07-07)

In the case of Karnataka, Professor Shamsundar of CREST, and his associate and friend Balachandran Chidambaranatraj, an architect, stepped up to offer a solution [109–111]. One requirement of the act was for the government to provide *anganwadis*, public childcare centers which integrate nutrition, health, and education. Balachandran proposed a method for constructing anganwadis using locally sourced materials including bamboo and mud. Working with Shamsundar, they submitted a proposal to construct such structures in 13 tribal hadis. The proposal was accepted, and construction of the first bamboo anganwadi begin in 2015. Pictures of the second anganwadi, completed in 2016, are shown in fig. 5.8.

In conjunction with construction of anganwadis, Professor Shamsundar also proposed construction of a microgrid within one of the 13 hadis where anganwadis will be constructed. To support the proposal, visits to three of the hadis were conducted to determine suitability. All three sites are located close to the borders of the protected areas, and thus are relatively accessible by road. Each hamlet consisted of roughly 20 homes with about five members each. None of the households have electric connections, generators, or any other source of electricity. Biomass is the main source of fuel for cooking, and candles or battery operated flashlights are used for lighting.

Based on the site visits, any of the three hadis could serve as a good candidate for a microgrid. Centralized components of the system could be located at the andganwadis. Due to the nature of home construction, rooftop PV would not likely be feasible: the homes seen consisted of clay or wattle construction with tile or tarp roofs (see fig. 5.9). As such, a pole- or frame-mounted PV array would be more suitable.

FIGURE 5.9: Typical homes in the tribal hadis (photos by author, 2016-07-07)

Due to the preliminary nature of the visits, additional details about individual homes were not collected. However, a GPS layout of the second two hadis visited was made (see fig. 5.10). The map was created in Google My Maps, and can be viewed on-line (with additional photos) at: `https://goo.gl/7L5iiI`.

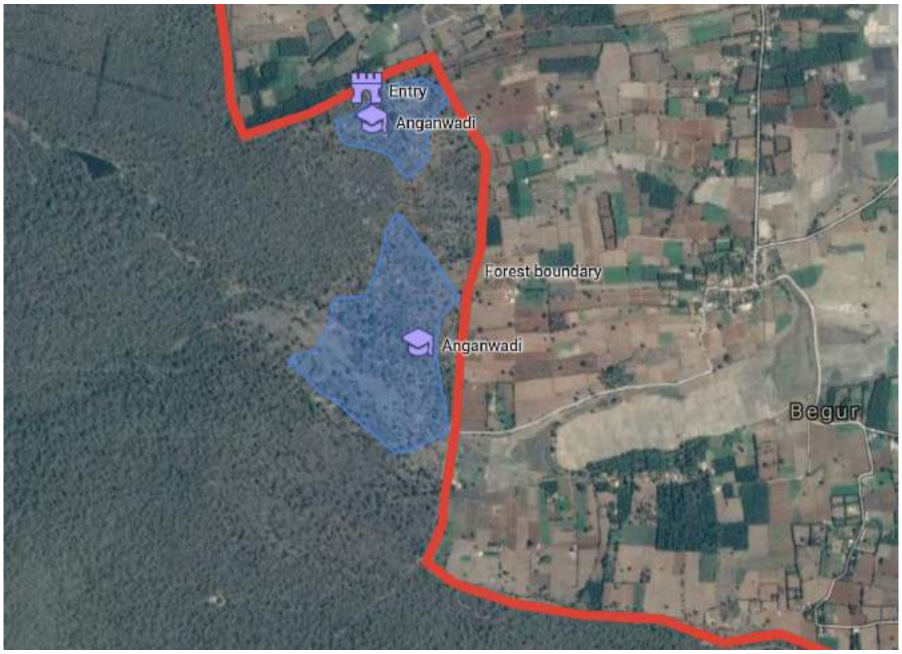

FIGURE 5.10: Map of two tribal hadis (outlined in blue) being considered for microgrid installation. View on-line: https://goo.gl/7L5iiI. Map data: Google Imagery, CNES / Astrium, CNES / Spot Image, DigitalGlobe (2017).

5.6.2 Semi-rural villages on the outskirts of Bengaluru

During the third trip to Mysuru the author accompanied Professor Shamsundar on a visit to two semi-rural villages just east of Bengaluru (the capital of the state of Karnataka). The two villages were Banandur (N12°46.5′ E77°23.9′) and Chowkahalli (N12°44.25′ E77°24.75′).

The visits were arranged through a mutual contact with the Bosch India Foundation, a branch of Bosch India which focuses on corporate social responsibility work in villages surrounding Bosch locations [112]. Banandur and Chowkahalli are both located near Bosch's Bidadi plant in the Bidadi Industrial area (see fig. 5.11).

While both villages, being located near the industrial park, have relatively reliable electric connections, there may be some opportunity for microgrid systems. In particular, both villages have very active dairy cooperatives, producing around 2,000 L of milk daily. Currently both cooperatives have diesel generators to provide back-up power for the dairy chillers. Installation of a microgrid in these areas could thus provide more sustainable back-up power during outages, while also reducing fuel costs. Both dairy cooperatives are located near other businesses and organizations (such as temples, stores, community centers, and a water purification facility) which could also benefit from a microgrid.

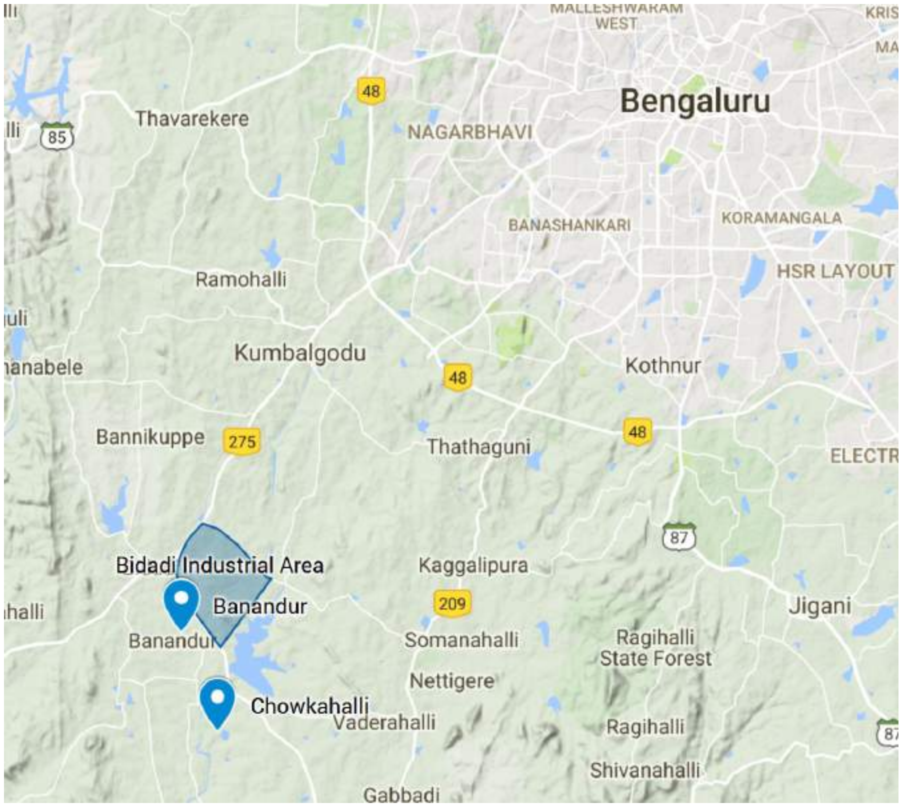

FIGURE 5.11: Map of villages visited with Bosch India Foundation. Map data: Google (2017).

At this time Professor Shamsundar is proposing to work with Bosch India Foundation and the villages to implement rainwater harvesting facilities. Other sustainable technologies, including microgrids, would be considered at a later date.

Chapter 6

Conclusions and future work

FIGURE 6.1: The famous Palace of Mysuru (photo by author, 2017-07-17)

6.1 Conclusions

The history of the electric grid is rooted in systems which resemble dc microgrids, an area of growing interest and research today. As an alternative to grid expansion and stand-alone power systems, microgrids enable a more rapid, cost-effective, and intelligent means for expanding electrification in the developing world. At the same time, the ancillary benefits of microgrids enable them to strengthen and improve existing centralized grids.

The control systems required for microgrids include the possibility of easily integrating renewables. This results in both cost savings and reduction of harmful emissions. Developments in dc microgrid research promise to lower the barriers to renewable energy integration even further, as dc microgrids are well-suited to integration with solar PV, batteries, and many types of loads, all of which are inherently dc systems.

To this end, the present study has contributed to development of a simple hardware interface for monitoring and controlling small dc "homegrids," called MEM–Microgrid Energy Manager. The ability of this system to monitor battery charge was tested. One of the core benefits of microgrids–the ability to intelligently share power–was also tested. Results indicate that MEM can preserve battery charge to make sure priority loads are powered, and that a pair of homegrids can effectively consolidate their local storage resources for mutual benefit.

Over three visits to the National Institute of Engineering in Mysuru, India, work was completed to develop a microgrid testbed for MEM. Energy sources including solar, wind, water, and bio-diesel were established for the Centre for Renewable Energy and Sustainable Technologies. Four small microgrid testbeds were established, and groundwork was done for eventually powering the entire office on the microgrid with renewable sources. Several site visits to find candidate locations for future microgrid projects were also conducted.

6.2 Future work

6.2.1 MEM system development

Work continues to improve and expand upon the MEM system. At the time of writing, an ac interface, corollary to HEMdc, had been developed and was being tested. Additional work is being done to allow one HEM system to monitor and control a mix of ac and dc loads and sources.

Work to make MEM ready for use outside of the laboratory is also being conducted. This includes development of a local user interface and a battery back-up module to run the hardware independent of the storage system for the loads HEM operates.

Extensive work on MEMcloud is also being conducted. Currently the software capabilities of MEMcloud do not reach the potential of the hardware, but development work underway is quickly rectifying this situation.

Finally, to allow MEM to reach a wider audience, the core team at UW-Madison is working to partition the software running on HEMapp–core software for operating the hardware peripherals and communicating with MEMcloud will be separated from software handling the decision-making and operations of the system. In this way, MEM system development and research on microgrid control can proceed on separate pathways.

6.2.2 Microgrid at CREST

Next steps at CREST will require completion of HEMac. Once this system is ready, the entirety of the loads at CREST can be moved on to the microgrid, giving the office the benefit of using reliable and renewable energy, and providing the research groups at UW-Madison and NIE with a real-world test bed for studying microgrids in general, and the MEM system specifically.

Integration of additional energy sources also needs to be completed. This includes interfacing with the 10 kW solar system at the NIE library to allow for power sharing with the CREST microgrid, and installing a change-over switch in CREST to allow for remotely operated selection of back-up sources between grid power and the bio-diesel generator.

Additional work developing remote sites is also needed. The challenges of building a power system in remote, tribal villages will need to be considered, and a long-term maintenance plan will be necessary.

To effectively plan and manage these projects, a core group of NIE students with dedicated electrical engineering faculty supervision will likely be required.

Appendix A

HEMdc Interface schematics

The HEMdc schematics and PCB layout were prepared in Altium Designer version 17.0.11 (Build 656). The source files are available on Gitlab at: https://gitlab.com/microgridenergymanager/HEM_DC_Interface. The repository includes the necessary files to build and populate the board, as well as instructions for constructing the cable required to interface with HEMcore.

Full schematics begin on the following page.

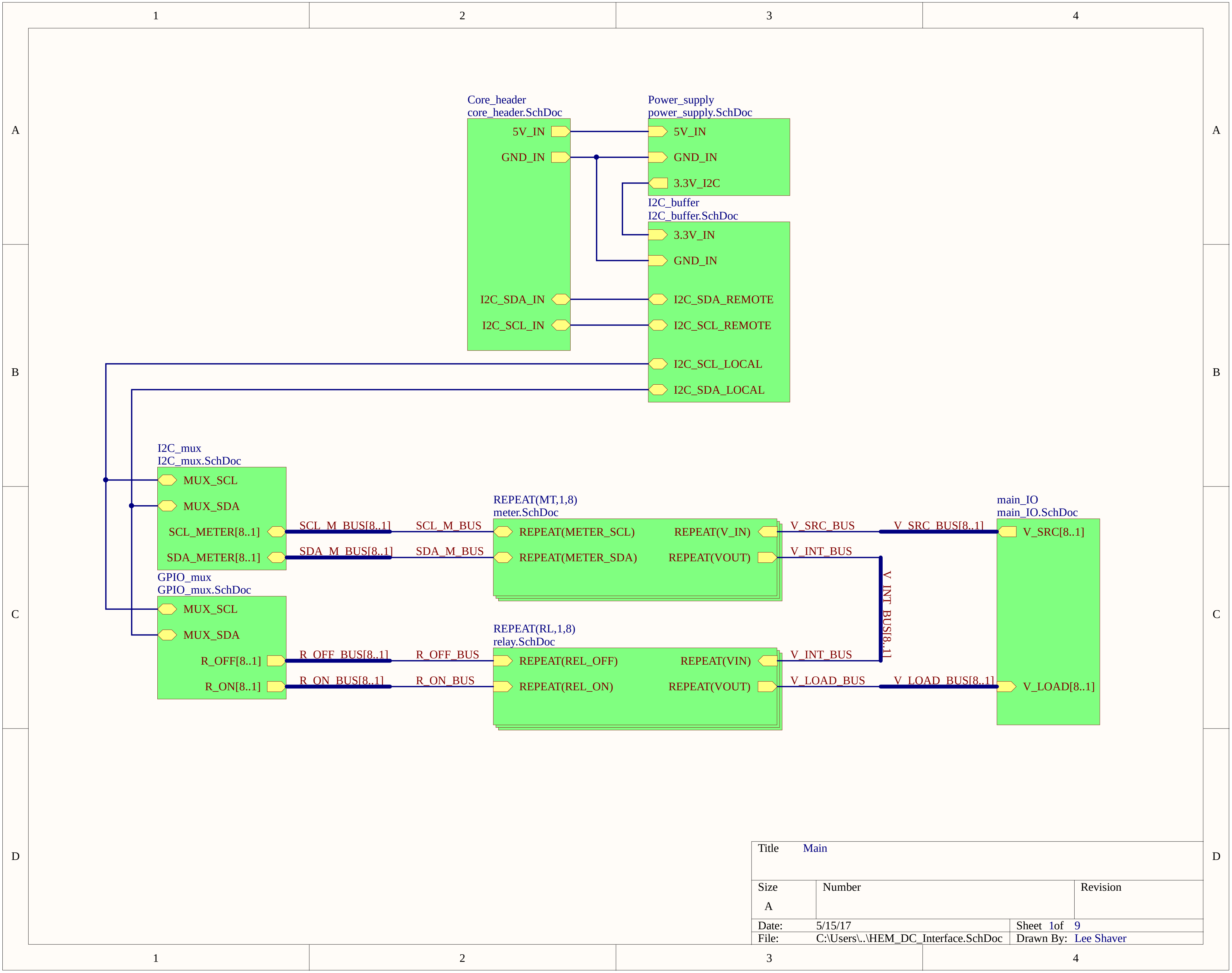

Core_header
core_header.SchDoc
5V_IN
GND_IN
I2C_SDA_IN
I2C_SCL_IN
Power_supply
power_supply.SchDoc
5V_IN
GND_IN
3.3V_I2C
I2C_buffer
I2C_buffer.SchDoc
3.3V_IN
GND_IN
I2C_SDA_REMOTE
I2C_SCL_REMOTE
I2C_SCL_LOCAL
I2C_SDA_LOCAL
I2C_mux
I2C_mux.SchDoc
MUX_SCL
MUX_SDA
SCL_METER[8..1]
SDA_METER[8..1]
GPIO_mux
GPIO_mux.SchDoc
MUX_SCL
MUX_SDA
R_OFF[8..1]
R_ON[8..1]
SCL_M_BUS[8..1]
SCL_M_BUS
SDA_M_BUS[8..1]
SDA_M_BUS
R_OFF_BUS[8..1]
R_OFF_BUS
R_ON_BUS[8..1]
R_ON_BUS
REPEAT(MT,1,8)
meter.SchDoc
REPEAT(METER_SCL)
REPEAT(METER_SDA)
REPEAT(V_IN)
REPEAT(VOUT)
REPEAT(RL,1,8)
relay.SchDoc
REPEAT(REL_OFF)
REPEAT(REL_ON)
REPEAT(VIN)
REPEAT(VOUT)
V_SRC_BUS
V_SRC_BUS[8..1]
V_INT_BUS
V_INT_BUS[8..1]
V_INT_BUS
V_LOAD_BUS
V_LOAD_BUS[8..1]
main_IO
main_IO.SchDoc
V_SRC[8..1]
V_LOAD[8..1]
Title Main
Size A
Number
Revision
Date: 5/15/17
Sheet 1of 9
File: C:\Users\..\HEM_DC_Interface.SchDoc
Drawn By: Lee Shaver

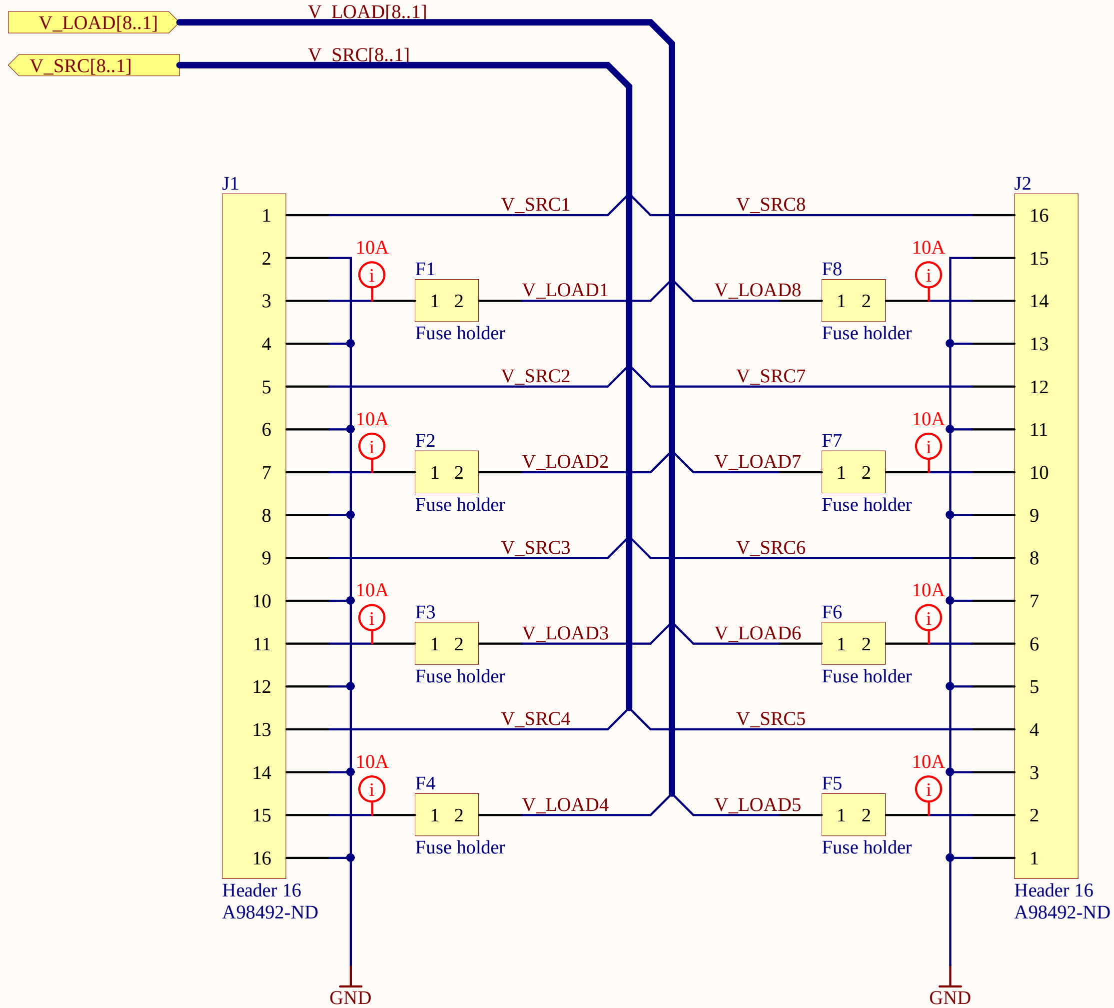

Title	Power, load, and communication interfaces		
Size: A	Number		Revision
Date: 5/15/17		Sheet 2 of 9	
File: C:\Users\..\main_IO.SchDoc		Drawn By: Lee Shaver	

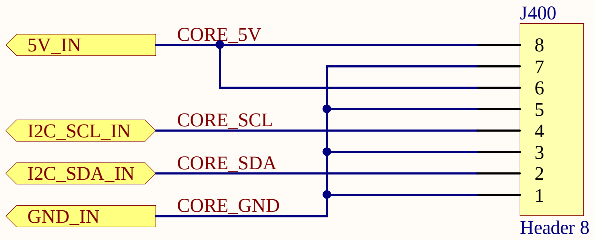

Title	HEM Core interface header		
Size A	Number		Revision
Date:	5/15/17	Sheet 3 of 9	
File:	C:\Users\..\core_header.SchDoc	Drawn By:	Lee Shaver

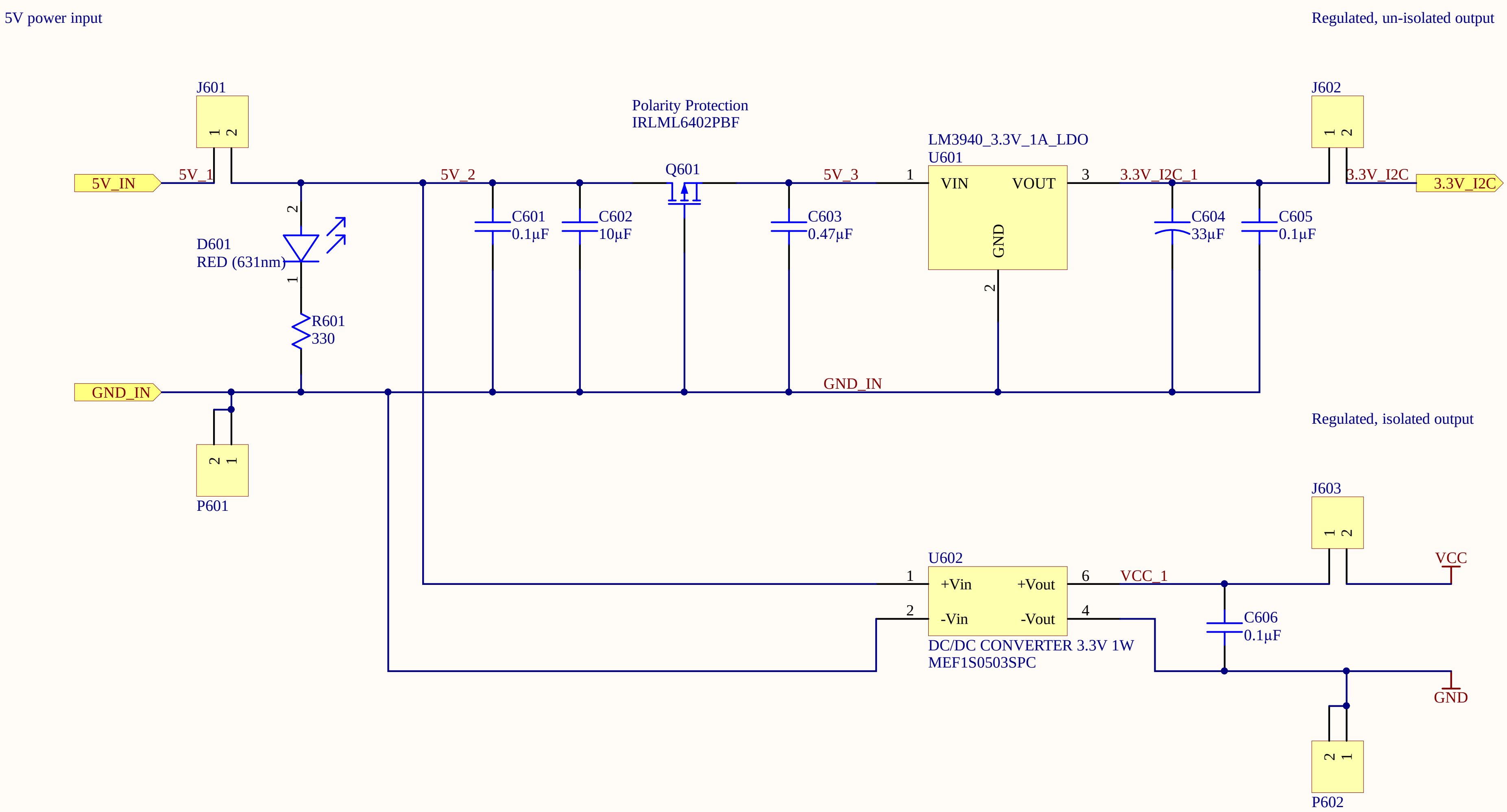

Title	DC Power Supply		
Size A	Number		Revision
Date:	5/15/17	Sheet 4 of 9	
File:	C:\Users\..\power_supply.SchDoc	Drawn By:	Lee Shaver

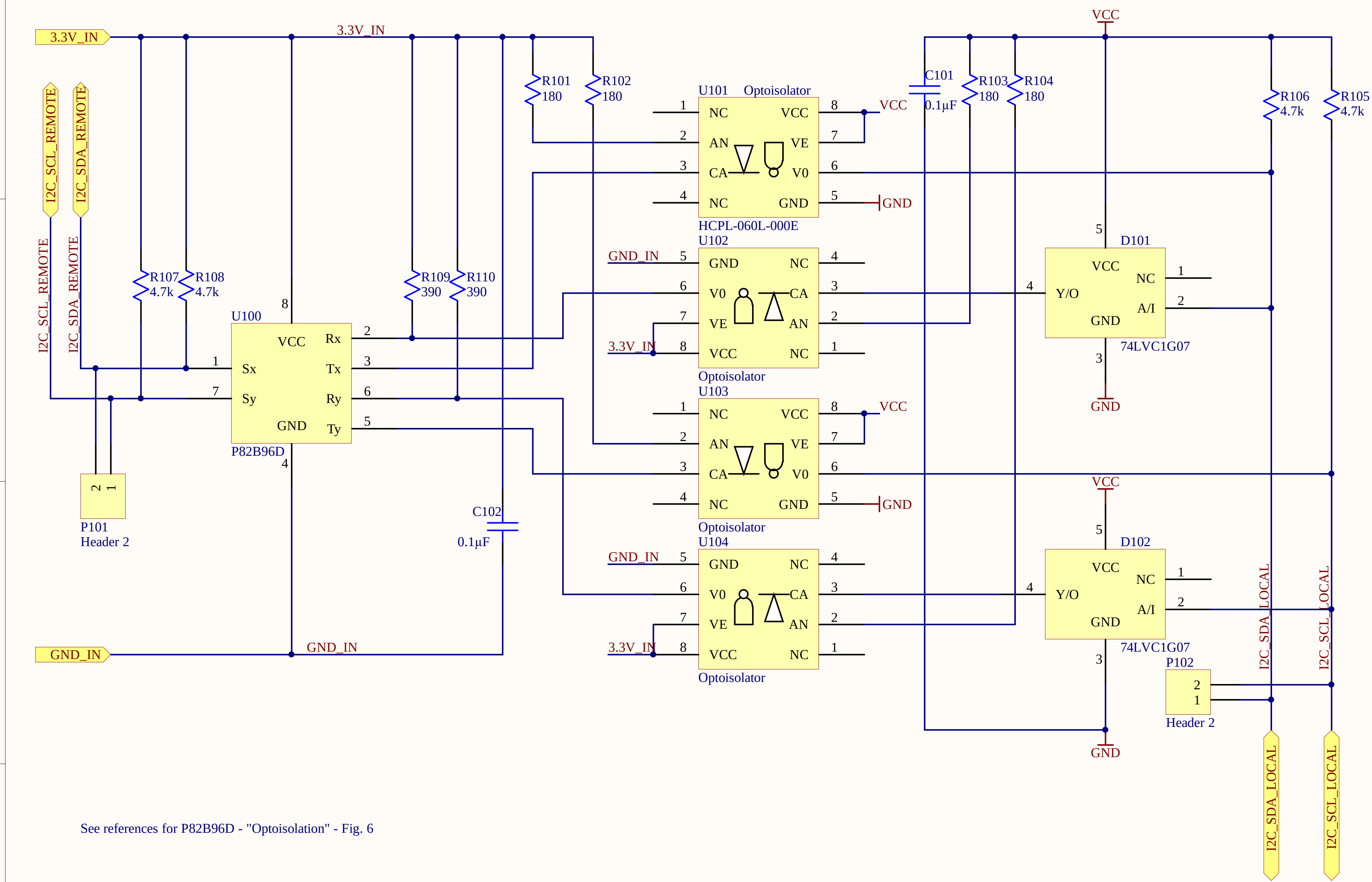

See references for P82B96D - "Optoisolation" - Fig. 6

Title	I2C booster and isolation		
Size A	Number		Revision
Date: 5/15/17		Sheet 5 of 9	
File: C:\Users\..\I2C_buffer.SchDoc		Drawn By: Lee Shaver	

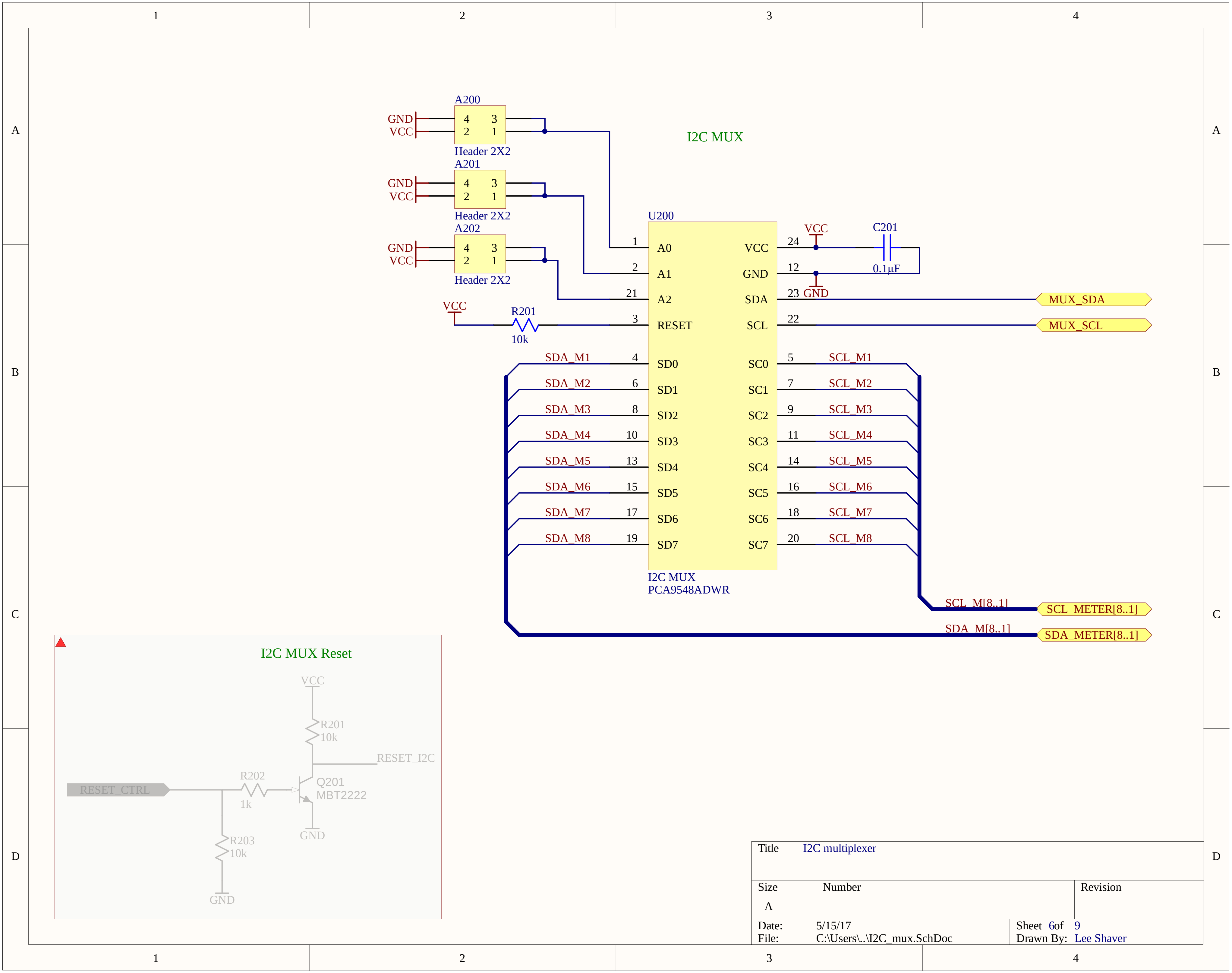

I2C MUX
A200
A201
A202
GND
VCC
4 3
2 1
Header 2X2
U200
A0
A1
A2
RESET
VCC
GND
SDA
SCL
SD0
SD1
SD2
SD3
SD4
SD5
SD6
SD7
SC0
SC1
SC2
SC3
SC4
SC5
SC6
SC7
I2C MUX
PCA9548ADWR
C201
0.1µF
R201
10k
MUX_SDA
MUX_SCL
SDA_M1
SDA_M2
SDA_M3
SDA_M4
SDA_M5
SDA_M6
SDA_M7
SDA_M8
SCL_M1
SCL_M2
SCL_M3
SCL_M4
SCL_M5
SCL_M6
SCL_M7
SCL_M8
SCL_M[8..1]
SCL_METER[8..1]
SDA_M[8..1]
SDA_METER[8..1]
I2C MUX Reset
VCC
R201
10k
RESET_I2C
R202
1k
Q201
MBT2222
RESET_CTRL
R203
10k
GND
Title I2C multiplexer
Size A
Number
Revision
Date: 5/15/17
Sheet 6of 9
File: C:\Users\..\I2C_mux.SchDoc
Drawn By: Lee Shaver

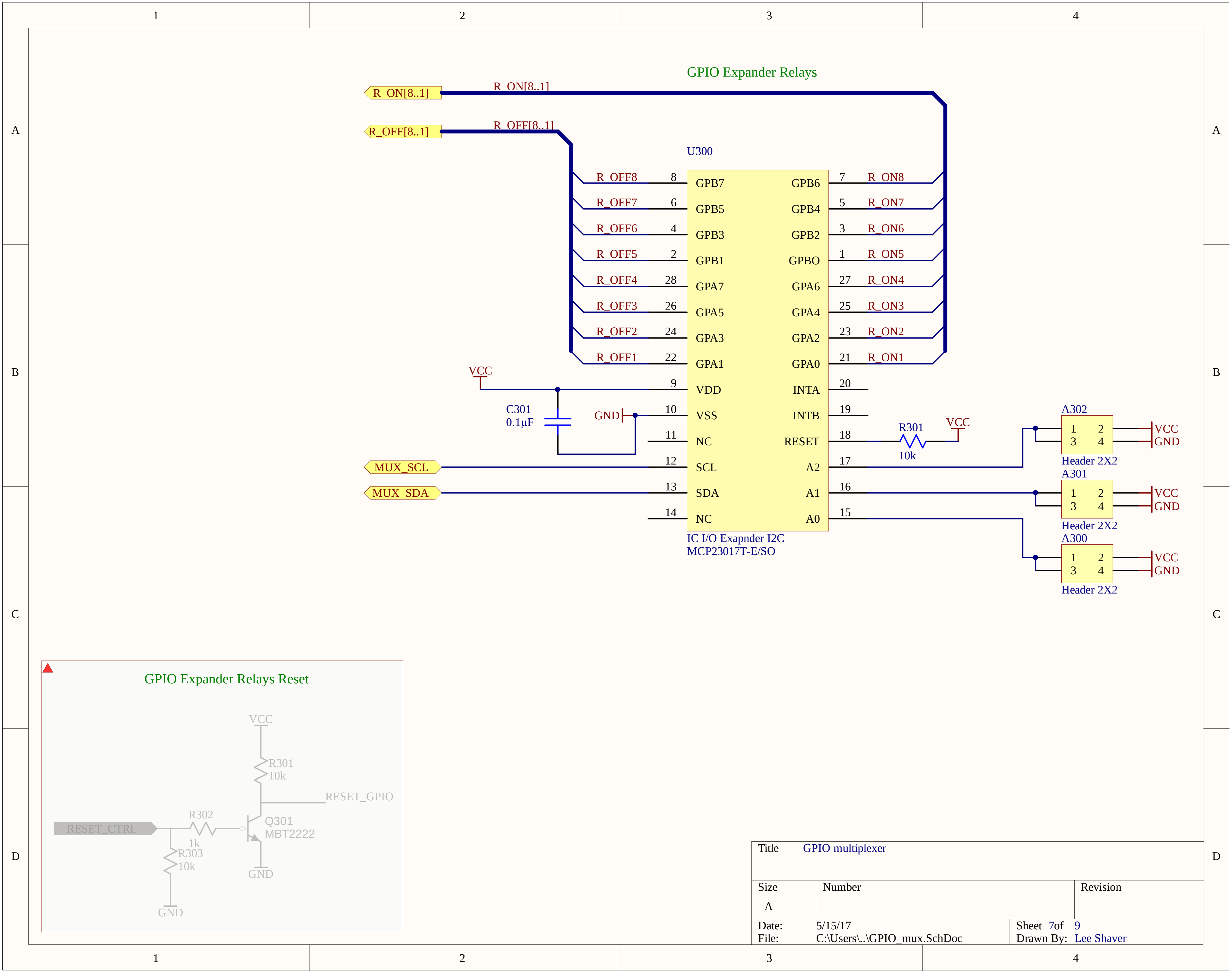
GPIO Expander Relays
R_ON[8..1]
R_OFF[8..1]
U300
R_OFF8 8 GPB7
R_OFF7 6 GPB5
R_OFF6 4 GPB3
R_OFF5 2 GPB1
R_OFF4 28 GPA7
R_OFF3 26 GPA5
R_OFF2 24 GPA3
R_OFF1 22 GPA1
GPB6 7 R_ON8
GPB4 5 R_ON7
GPB2 3 R_ON6
GPBO 1 R_ON5
GPA6 27 R_ON4
GPA4 25 R_ON3
GPA2 23 R_ON2
GPA0 21 R_ON1
VCC
9 VDD
INTA 20
C301
0.1µF
GND
10 VSS
INTB 19
11 NC
RESET 18
R301
10k
VCC
MUX_SCL
12 SCL
A2 17
MUX_SDA
13 SDA
A1 16
14 NC
A0 15
IC I/O Exapnder I2C
MCP23017T-E/SO
A302
1 2
3 4
VCC
GND
Header 2X2
A301
1 2
3 4
VCC
GND
Header 2X2
A300
1 2
3 4
VCC
GND
Header 2X2
GPIO Expander Relays Reset
VCC
R301
10k
RESET_GPIO
RESET_CTRL
R302
1k
Q301
MBT2222
R303
10k
GND
GND
Title GPIO multiplexer
Size A
Number
Revision
Date: 5/15/17
Sheet 7of 9
File: C:\Users\..\GPIO_mux.SchDoc
Drawn By: Lee Shaver

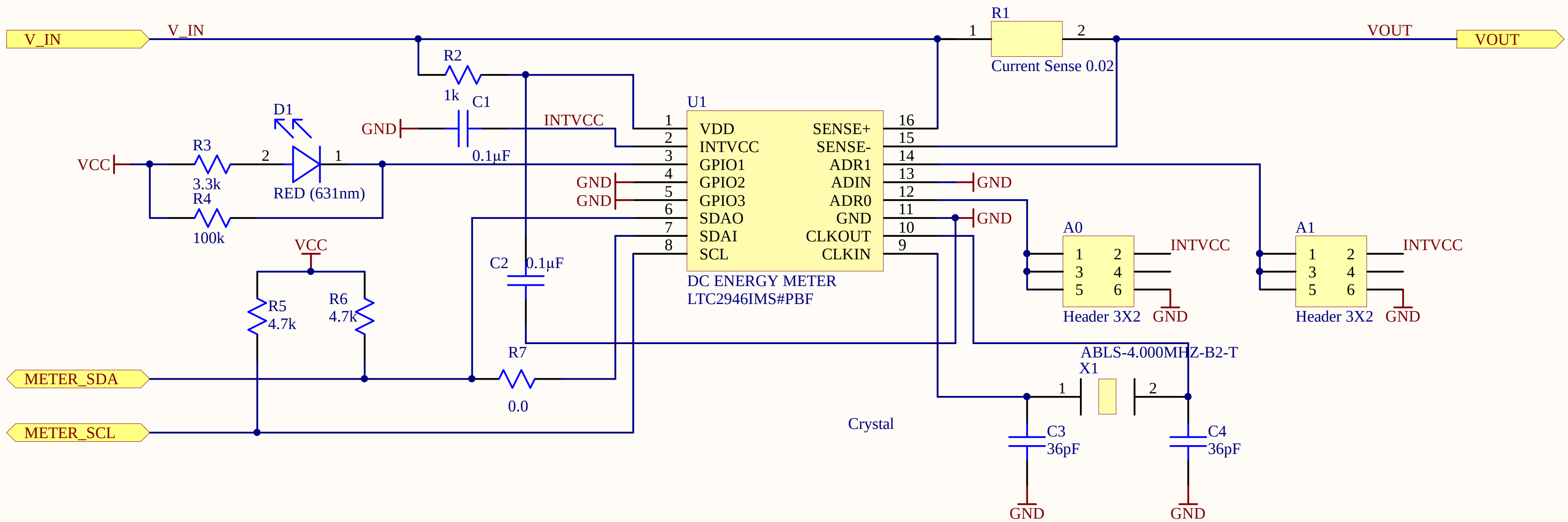

Title	DC meter	
Size A	Number	Revision
Date: 5/15/17		Sheet 8 of 9
File: C:\Users\..\meter.SchDoc		Drawn By: Lee Shaver

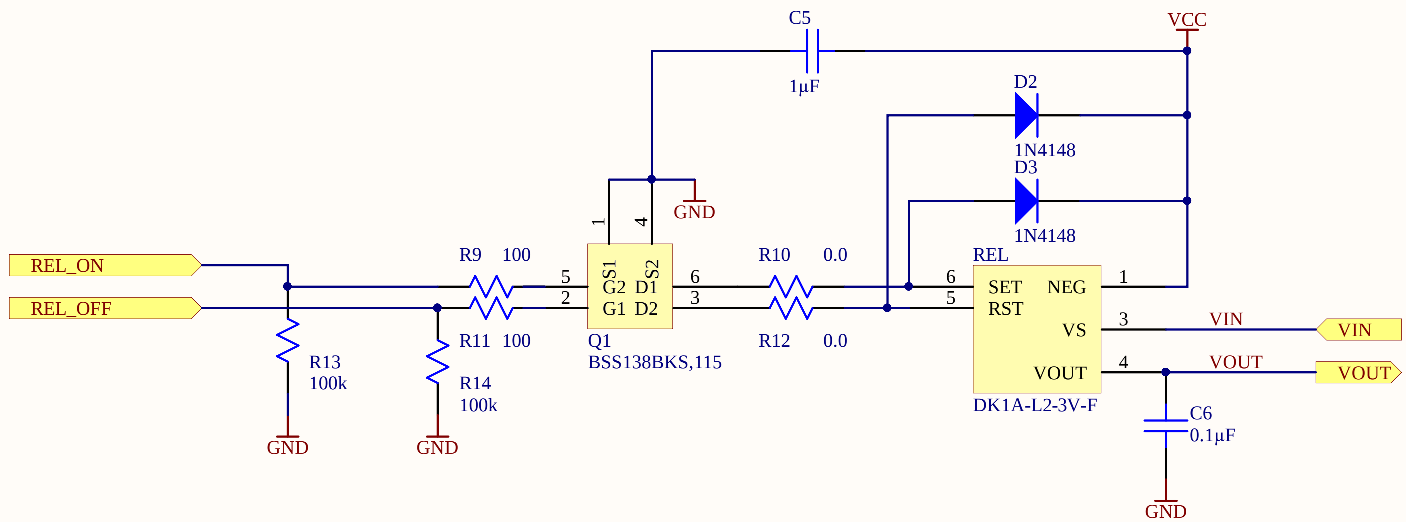

Title	Relay		
Size A	Number		Revision
Date: 5/15/17		Sheet 9 of 9	
File: C:\Users\..\relay.SchDoc		Drawn By: Lee Shaver	

Appendix B

Code reference for HEMdc experiments

This appendix provides a reference for the code used to run the experiments in chapter 4.

The most recent version of HEMapp includes the function `dcGetStateofCharge()` for monitoring battery SOC. The code is maintained in the HEMapp repository, available at https://gitlab.com/microgridenergymanager/hemapp (permission to access the project should be requested from the current master developer). This repository is actively maintained and updated as new features and bugfixes are implemented.

B.1 Individual battery management

The `batteryMonitor()` thread of the `main.c` file of HEMapp was used to implement the individual battery management experiment as described in this report. Shortly after the experiment was concluded, the functionality was moved from the HEMapp C code into a Python script, which was also used for the collective battery management experiments. Python scripting is discussed in appendix B.3.

For reference, a snippet of the C code is provided below, showing a simple method for implementing load prioritization:

```
if( presentSOC <= 75 )
{
        if( presentSOC <= 50 )
        {
                if( getNodeRelayStatus(0) == 1 )
                {
                        relayActuate(RELAY0_OFF))
                        setNodeRelayStatus(0,0);
                }
        }
        else if( presentSOC <= 25 )
        {
                if( getNodeRelayStatus(2) == 1 )
```

```
                {
                        relayActuate(RELAY2_OFF))
                        setNodeRelayStatus(2,0);
                }
        }
        else if ( getNodeRelayStatus(1) == 1 )
        {
                relayActuate(RELAY1_OFF))
                setNodeRelayStatus(1,0);
        }
}
```

In this example, the priority of the three nodes (0, 1, and 2) is known ahead of time, as well as the priority thresholds. Improvements to the code would generalize these values so that users and/or MEMcloud could change the values on-the-fly.

B.2 Collective battery management

The collective battery management experiment was implemented using Python scripting. As of this writing, the most current version of HEMapp includes the necessary functions to run and communicate with a running Python script, as described in appendix B.3.

The Python script used for the experiment is available at https://gitlab.com/lshaver/thesis/blob/export_test/scripts/export.py. A snippet of the code is provided below to illustrate the functionality:

```python
def prioritize():

      while True:

            if ( SOC <= 10 ):
                  # Turn off the high priority load
                  toggleRelay( relayHigh, 'off' )

            elif ( SOC <= 40 ):
                  # Turn off the medium priority load
                  toggleRelay( relayMed, 'off' )

            elif ( SOC <= 50 ):
                  if importing is False:
                        # Request power import
                        sendToServer(exportCommand)
                        importing = True
                        # Turn on the relay which will allow input power
                        toggleRelay( relayLink, 'on' )

            elif ( SOC <= 60 ):
```

```
                if exporting is True:
                    # Turn off the relay which would allow output power
                    toggleRelay( relayLink, 'off' )
                    exporting = False

            elif ( SOC <= 70 ):
                # Turn off the low piority load
                toggleRelay( relayLow, 'off' )

            time.sleep(5)
```

In this example, thresholds are known ahead of time, while load priorities (`relayHigh`, for example) are set by a simple header file. Future improvements will allow users and/or MEMcloud to set these values on-the-fly.

B.3 Python scripting

On any HEMcore or HEMdc system running up-to-date HEMapp code, a Python script can easily be implemented; only a few lines of code are necessary to create the links between HEMapp and the Python script:

```
import socket
SERVER_ADDRESS = 8888
sock = socket.socket(socket.AF_INET, socket.SOCK_DGRAM)
server_address = ('localhost', SERVER_ADDRESS)
```

Then, the following lines can be used to send or receive some `data` from HEMapp:

```
# Sending
sent = sock.sendto(data, server_address)
# Receiving
data, server = sock.recvfrom(4096)
```

As this functionality is developed further, additional examples will be made available in the main HEMapp repository on Gitlab.

Appendix C

CREST office and microgrid testbed wiring

Figure C.1 provides a simplified one-line diagram of the CREST office, showing the type and rating of loads used.

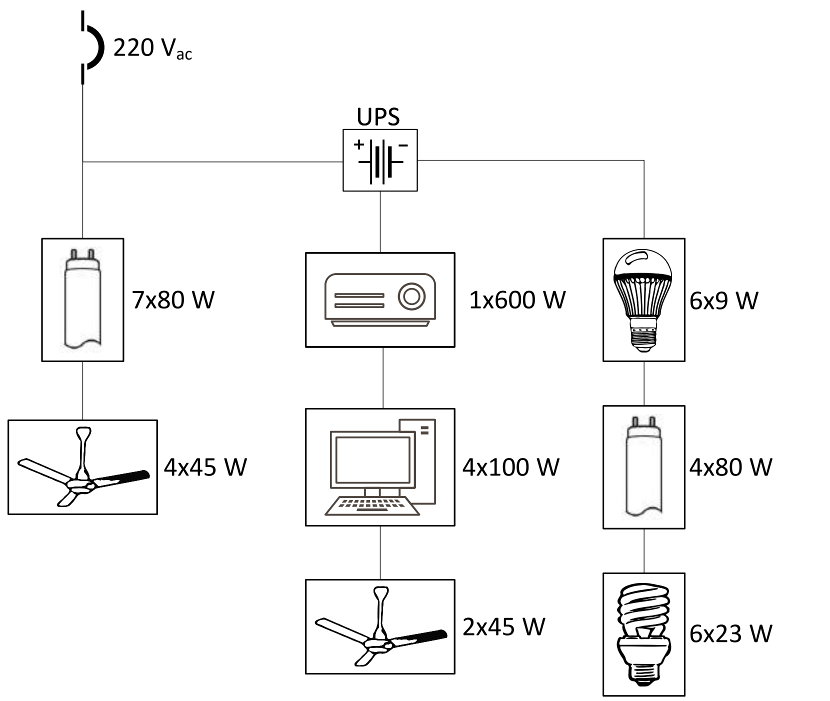

FIGURE C.1: A simplified one-line diagram of CREST office loads

Figure C.2 gives the CREST floor-plan and a basic electrical layout. Different colors are used to indicate the different circuits in the office:

Red: Lights and fans, connected to mains power only.

Yellow: Main UPS circuit, which feeds the projector, two sub-circuits (green and blue), and outlets on the north wall.

Green: UPS sub-circuit powering lights along the west wall.

Blue: UPS sub-circuit supplying lights and outlets along the east wall.

Purple: DC lighting circuit. The lights are fixed in the ceiling along the north wall. Input power from this circuit comes from the microgrid testbeds.

Switch and outlet banks refer to grouped switches and/or outlets permanently installed in the walls. Some of these also serve as junction boxes for other circuits: notably the easternmost outlet on the north wall, where the main UPS circuit (yellow) branches into the green and blue sub-circuits. Depending on requirements for rewiring the office, these junction boxes could be used to additionally sub-divide circuits.

The remaining figures in this chapter (figs. C.3 to C.6) as-built schematics of the four microgrid testbeds at CREST.

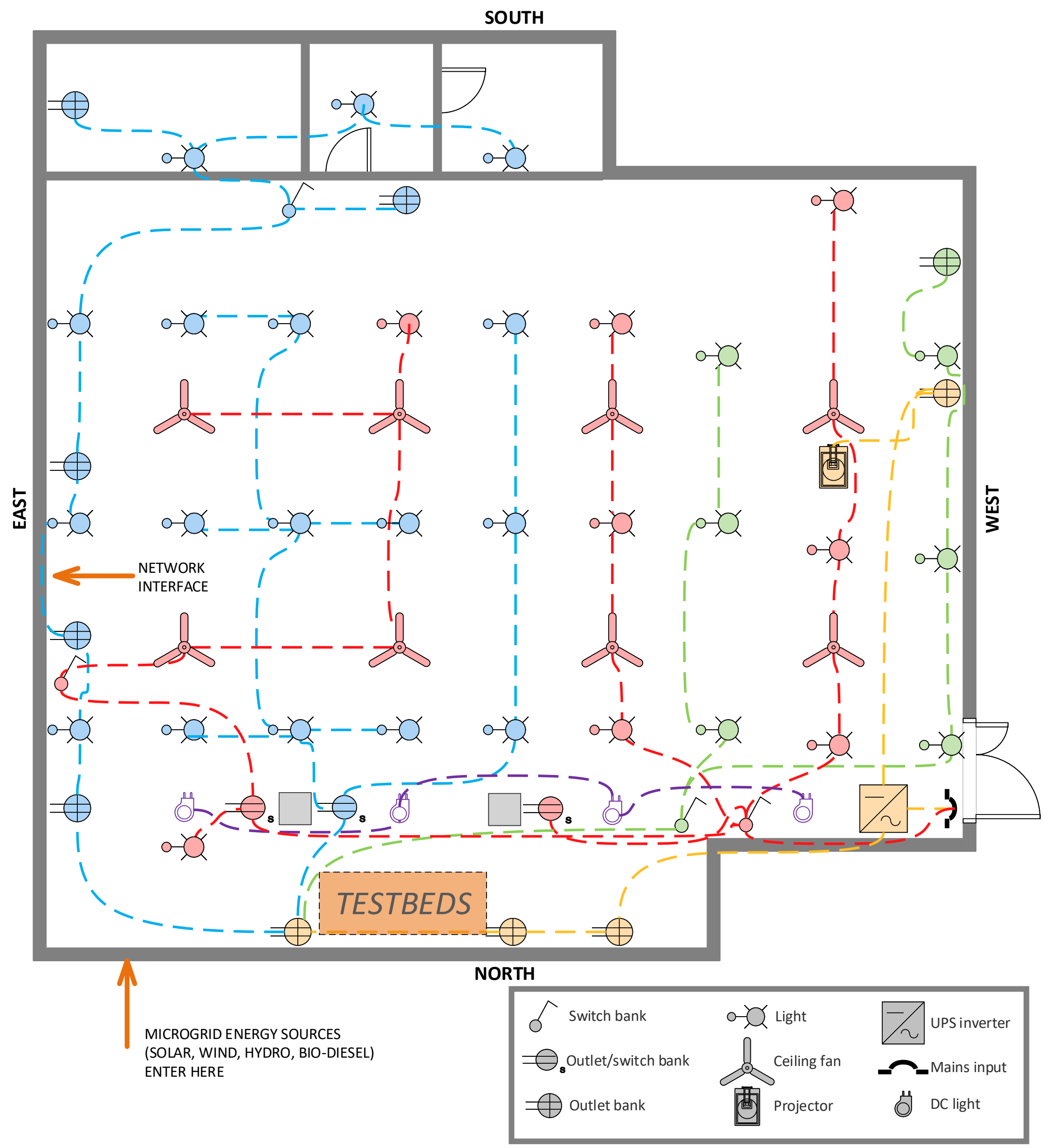

FIGURE C.2: Electrical layout of CREST

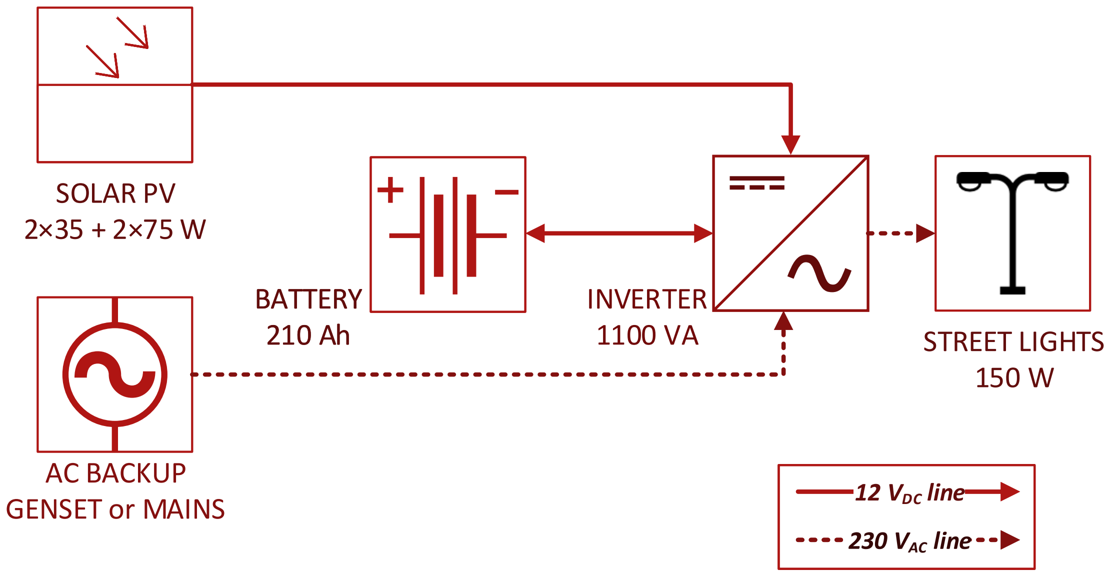

FIGURE C.3: Schematic of "red" microgrid testbed

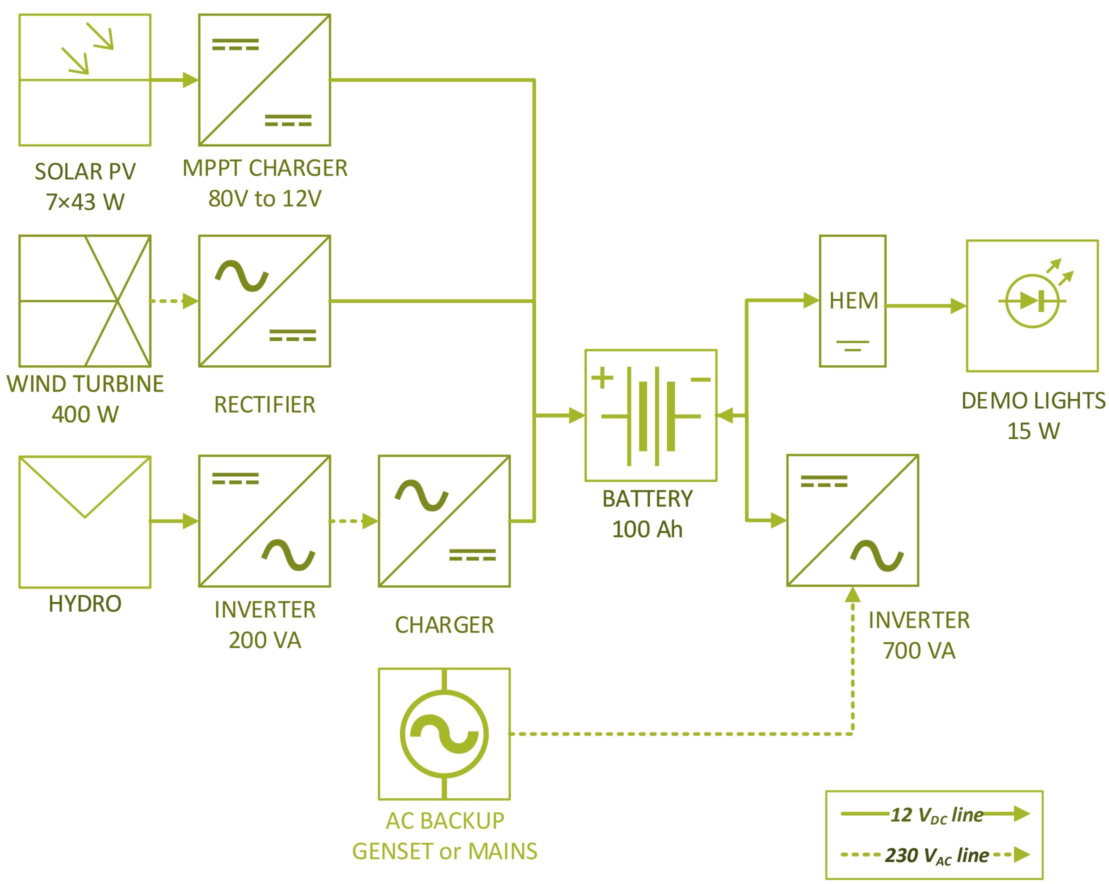

FIGURE C.4: Schematic of "green" microgrid testbed

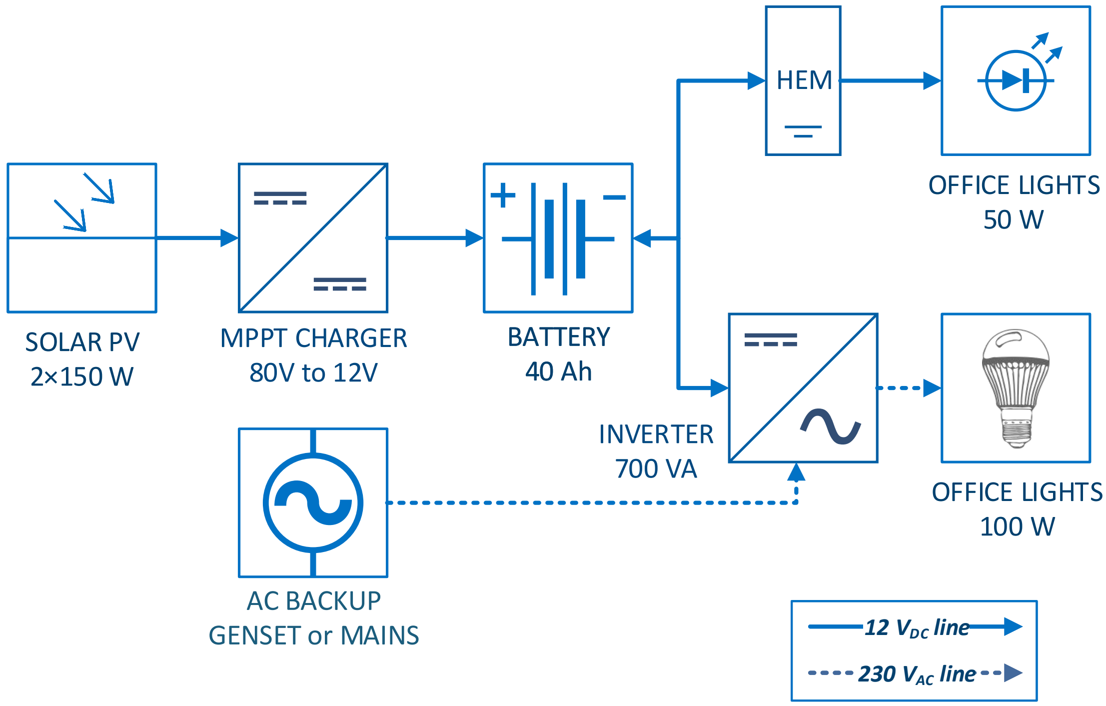

FIGURE C.5: Schematic of "blue" microgrid testbed

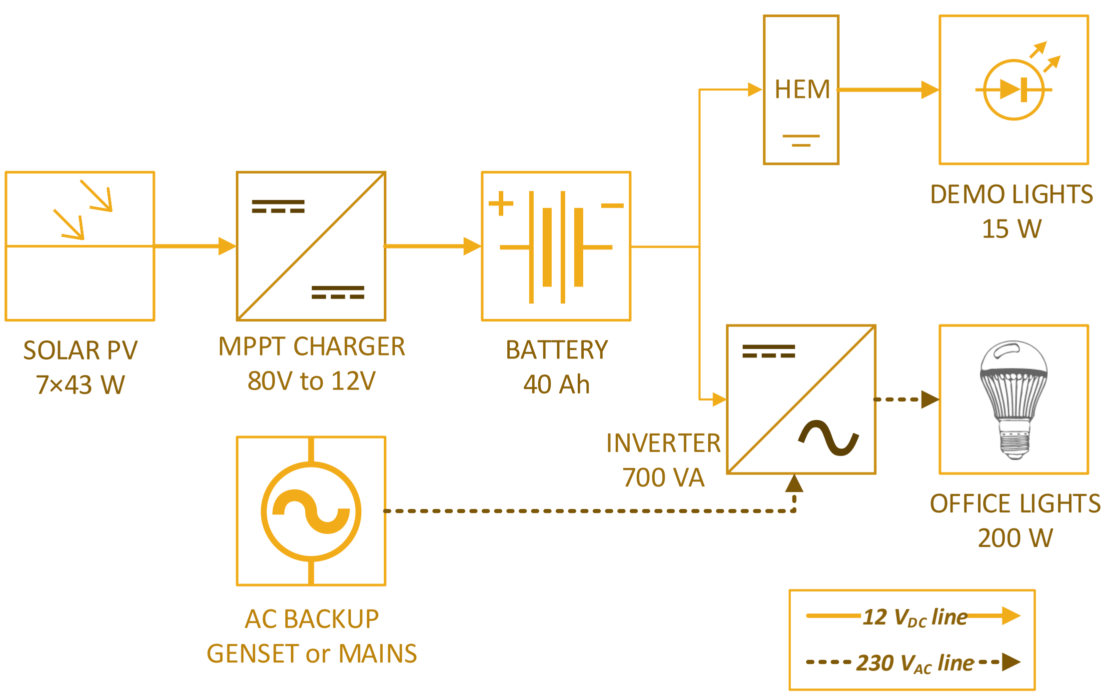

FIGURE C.6: Schematic of "yellow" microgrid testbed

Bibliography

[1] Earl Morter. *Pearl Street Station*. In: *Wikipedia*. 1890. URL: https://en.wikipedia.org/wiki/File:PearlStreetStation.jpg#filelinks.

[2] Ania Monaco. "Edison's Pearl Street Station Recognized With Milestone". In: *The Institute* (July 27, 2011). URL: http://theinstitute.ieee.org/tech-history/technology-history/edisons-pearl-street-station-recognized-with-milestone810.

[3] Richard F. Hirsh. *Emergence of Electrical Utilities in America*. Sept. 2002. URL: http://americanhistory.si.edu/powering/.

[4] R. W. Lobenstein and C. Sulzberger. "Eyewitness to Dc History". In: *IEEE Power and Energy Magazine* 6.3 (May 2008), pp. 84–90. ISSN: 1540-7977. DOI: 10.1109/MPE.2008.920421.

[5] Institute for Energy Research. *History of Electricity*. Aug. 29, 2014. URL: http://instituteforenergyresearch.org/history-electricity/.

[6] Union of Concerned Scientists. *How the Electricity Grid Works*. Feb. 18, 2015. URL: http://www.ucsusa.org/clean-energy/how-electricity-grid-works.

[7] Martin Doppelbauer. *A Short History of Electric Motors*. Sept. 25, 2014. URL: https://www.eti.kit.edu/english/1376.php.

[8] Stephanie Joyce. *When The Largest Machine In The World Fails*. May 16, 2015. URL: http://insideenergy.org/2015/05/16/when-the-largest-machine-in-the-world-fails/.

[9] Sonia Aggarwal. *Greasing the Electric Grid, the World's Largest Machine (Op-Ed)*. Nov. 24, 2014. URL: http://www.livescience.com/48893-improving-efficiency-on-the-electric-grid.html.

[10] Jean-Baptiste Michel et al. "Quantitative Analysis of Culture Using Millions of Digitized Books". In: *Science* 331.6014 (Jan. 14, 2011), pp. 176–182. ISSN: 0036-8075. DOI: 10.1126/science.1199644. URL: http://science.sciencemag.org.ezproxy.library.wisc.edu/content/331/6014/176.

[11] The Google Books Team. *Google Books Ngram Viewer*. 2013. URL: https://books.google.com/ngrams.

[12] Energy and Environmental Research Center. *Demonstration of Technologies for Remote Power Generation in Alaska*. Semi-Annual Report Task 3.14. Energy and Environmental Research Center, Aug. 11, 1997. URL: https://www.osti.gov/scitech/servlets/purl/650240.

[13] Chris Marnay, F. Javier Rubio, and Afzal S. Siddiqui. "Shape of the Microgrid". In: *Lawrence Berkeley National Laboratory* (Nov. 1, 2000). URL: http://escholarship.org/uc/item/9fw029wb.

[14] D. Herman. "Investigation of the Technical and Economic Feasibility of Micro-Grid-Based Power Systems". In: *Electric Power Research Institute, Palo Alto, CA* 2 (2001), pp. 1–1. URL: http://assets.fiercemarkets.net/public/smartgridnews/EPRI_Technical_Report_Micro-Grid.pdf.

[15] R. H. Lasseter. "MicroGrids". In: *2002 IEEE Power Engineering Society Winter Meeting. Conference Proceedings (Cat. No.02CH37309)*. 2002 IEEE Power Engineering Society Winter Meeting. Conference Proceedings (Cat. No.02CH37309). Vol. 1. 2002, 305–308 vol.1. DOI: 10.1109/PESW.2002.985003.

[16] R. H. Lasseter and P. Paigi. "Microgrid: A Conceptual Solution". In: *2004 IEEE 35th Annual Power Electronics Specialists Conference (IEEE Cat. No.04CH37551)*. 2004 IEEE 35th Annual Power Electronics Specialists Conference (IEEE Cat. No.04CH37551). Vol. 6. June 2004, 4285–4290 Vol.6. DOI: 10.1109/PESC.2004.1354758.

[17] Dan T. Ton and Merrill A. Smith. "The US Department of Energy's Microgrid Initiative". In: *The Electricity Journal* 25.8 (2012), pp. 84–94. URL: http://www.sciencedirect.com/science/article/pii/S1040619012002254.

[18] Krista Eastman. *From Micro to Macro, UW–Madison's Expansion of the Microgrid Idea*. Mar. 3, 2017. URL: https://energy.wisc.edu/news/micro-macro-uw-madisons-expansion-microgrid-idea.

[19] Microgrids at Berkeley Lab. *About Microgrids*. 2017. URL: https://building-microgrid.lbl.gov/about-microgrids.

[20] R. C. Dugan and S. K. Price. "Issues for Distributed Generation in the US". In: *2002 IEEE Power Engineering Society Winter Meeting. Conference Proceedings (Cat. No.02CH37309)*. 2002 IEEE Power Engineering Society Winter Meeting. Conference Proceedings (Cat. No.02CH37309). Vol. 1. 2002, 121–126 vol.1. DOI: 10.1109/PESW.2002.984969.

[21] R. Brent Alderfer et al. *Making Connections: Case Studies of Interconnection Barriers and Their Impact on Distributed Power Projects*. Case Study NREL/SR-200-28053. Golden, CO (US): National Renewable Energy Laboratory, July 2000. URL: http://www.osti.gov/scitech/biblio/753767.

[22] EPRI. *Development of a Standard Language for Photovoltaic and Storage Integration*. Technical Brief 1020435. Palo Alto, CA: Electric Power Research Institute, Dec. 2009. URL: http://www.epri.com/abstracts/Pages/ProductAbstract.aspx?ProductId=000000000001020435.

[23] IEEE Standards Board. *IEEE Standard for Interconnecting Distributed Resources with Electric Power Systems: 1547-2003*. New York: Institute of Electrical and Electronics Engineers, 2003. ISBN: 978-0-7381-3720-9.

[24] Berkeley Lab. *Examples of Microgrids*. 2017. URL: https://building-microgrid.lbl.gov/examples-microgrids.

[25] S. Morozumi. "Micro-Grid Demonstration Projects in Japan". In: *2007 Power Conversion Conference - Nagoya*. 2007 Power Conversion Conference - Nagoya. Apr. 2007, pp. 635–642. DOI: 10.1109/PCCON.2007.373032.

[26] N. W. A. Lidula and A. D. Rajapakse. "Microgrids Research: A Review of Experimental Microgrids and Test Systems". In: *Renewable and Sustainable Energy Reviews* 15.1 (Jan. 2011), pp. 186–202. ISSN: 1364-0321. DOI: 10.1016/j.rser.2010.09.041. URL: http://www.sciencedirect.com/science/article/pii/S136403211000328X.

[27] Mohammad Shahidehpour and Joseph F. Clair. "A Functional Microgrid for Enhancing Reliability, Sustainability, and Energy Efficiency". In: *The Electricity Journal* 25.8 (Oct. 2012), pp. 21–28. ISSN: 1040-6190. DOI: 10.1016/j.tej.2012.09.015. URL: http://www.sciencedirect.com/science/article/pii/S1040619012002278.

[28] B. Washom et al. "Ivory Tower of Power: Microgrid Implementation at the University of California, San Diego". In: *IEEE Power and Energy Magazine* 11.4 (July 2013), pp. 28–32. ISSN: 1540-7977. DOI: 10.1109/MPE.2013.2258278.

[29] Kevin B. Jones et al. "The Urban Microgrid: Smart Legal and Regulatory Policies to Support Electric Grid Resiliency and Climate Mitigation". In: *Fordham Urb. LJ* 41 (2013), p. 1695. URL: http://heinonline.org/hol-cgi-bin/get_pdf.cgi?handle=hein.journals/frdurb41&section=49.

[30] Julia Pyper. "Are Microgrids the Answer to City-Disrupting Disasters?" In: *Scientific American* (Sept. 11, 2013). URL: https://www.scientificamerican.com/article/are-microgrids-the-answer-to-city-disrupting-disasters/.

[31] Taha Selim Ustun, Cagil Ozansoy, and Aladin Zayegh. "Recent Developments in Microgrids and Example Cases around the World—A Review". In: *Renewable and Sustainable Energy Reviews* 15.8 (Oct. 2011), pp. 4030–4041. ISSN: 13640321. DOI: 10.1016/j.rser.2011.07.033. URL: http://linkinghub.elsevier.com/retrieve/pii/S1364032111002735.

[32] Robert Liam Dohn. "The Business Case for Microgrids". In: *White Paper Siemens* (2011). URL: http://w3.usa.siemens.com/smartgrid/us/en/microgrid/Documents/The%20business%20case%20for%20microgrids_Siemens%20white%20paper.pdf.

[33] Giri Venkataramanan and Chris Marnay. "A Larger Role for Microgrids". In: *IEEE Power and Energy Magazine* 6.3 (May 2008), pp. 78–82. ISSN: 1540-7977. DOI: 10.1109/MPE.2008.918720. URL: http://ieeexplore.ieee.org/lpdocs/epic03/wrapper.htm?arnumber=4505829.

[34] Daniel Schnitzer et al. *Microgrids for Rural Electrification: A Critical Review of Best Practices Based on Seven Case Studies*. Case Study. United Nations Foundation, Jan. 2014. URL: https://rael.berkeley.edu/wp-content/uploads/2015/04/MicrogridsReportEDS.pdf.

[35] Nathaniel J. Williams et al. "Enabling Private Sector Investment in Microgrid-Based Rural Electrification in Developing Countries: A Review". In: *Renewable and Sustainable Energy Reviews* 52 (Dec. 2015), pp. 1268–1281. ISSN: 1364-0321. DOI: 10.1016/j.rser.2015.07.153. URL: http://www.sciencedirect.com/science/article/pii/S136403211500800X.

[36] The World Bank. *Access to Electricity (% of Population)*. 2016. URL: http://data.worldbank.org/indicator/EG.ELC.ACCS.ZS.

[37] Vijay Modi et al. *Energy Services for the Millenium Development Goals*. Study. UN Millenium Project, World Bank, 2005. URL: http://www.unmillenniumproject.org/documents/MP_Energy_Low_Res.pdf.

[38] Sustainable Energy For All. *About Us | Sustainable Energy for All (SEforALL)*. 2016. URL: http://www.se4all.org/about-us.

[39] Sudeshna Ghosh Banerjee et al. *Global Tracking Framework 2013*. Progress Report. Washington, DC, USA: The World Bank, 2013. URL: http://trackingenergy4all.worldbank.org/~/media/GIAWB/GTF/Documents/GTF-2013-Full-Report.pdf.

[40] F. Fluitman. *Socio-Economic Impact of Rural Electrification in Developing Countries: A Review of Evidence*. ILO Working Paper 992274003402676. International Labour Organization, 1983. URL: https://ideas.repec.org/p/ilo/ilowps/992274003402676.html.

[41] Energy Sector Management Assistance Program. *Rural Electrification and Development in the Philippines: Measuring the Social and Economic Benefits*. Collaborative Study 255/03. Washington, DC, USA: World Bank, 2003. URL: http://siteresources.worldbank.org/INTPSIA/Resources/490023-1120845825946/philippines_rural_electrification.pdf.

[42] Independent Evaluation Group. *The Welfare Impact of Rural Electrification: A Reassessment of the Costs and Benefits*. Washington, DC, USA: The World Bank, 2008. ISBN: 978-0-8213-7367-5. URL: http://elibrary.worldbank.org/doi/book/10.1596/978-0-8213-7367-5.

[43] Independent Evaluation Group. *World Bank Group Support to Electricity Access, FY2000-2014*. Evaluation. IEG, 2015. URL: https://ieg.worldbankgroup.org/Data/reports/chapters/Electricity_Access_1.pdf.

[44] Todd Levin and Valerie M. Thomas. "Least-Cost Network Evaluation of Centralized and Decentralized Contributions to Global Electrification". In: *Energy Policy*. Modeling Transport (Energy) Demand and Policies 41 (Feb. 2012), pp. 286–302. ISSN: 0301-4215. DOI: 10.1016/j.enpol.2011.10.048. URL: http://www.sciencedirect.com/science/article/pii/S0301421511008639.

[45] Todd Levin and Valerie M. Thomas. "Can Developing Countries Leapfrog the Centralized Electrification Paradigm?" In: *Energy for Sustainable Development* 31 (Apr. 2016), pp. 97–107. ISSN: 0973-0826. DOI: 10.1016/j.esd.2015.12.005. URL: http://www.sciencedirect.com/science/article/pii/S0973082615301599.

[46] A. Chaurey and T. C. Kandpal. "A Techno-Economic Comparison of Rural Electrification Based on Solar Home Systems and PV Microgrids". In: *Energy Policy*. The Role of Trust in Managing Uncertainties in the Transition to a Sustainable Energy Economy, Special Section with Regular Papers 38.6 (June 2010), pp. 3118–3129. ISSN: 0301-4215. DOI: 10.1016/j.enpol.2010.01.052. URL: http://www.sciencedirect.com/science/article/pii/S0301421510000807.

[47] Uwe Deichmann et al. "The Economics of Renewable Energy Expansion in Rural Sub-Saharan Africa". In: *Energy Policy* 39.1 (Jan. 2011), pp. 215–227. ISSN: 0301-4215. DOI: 10.1016/j.enpol.2010.09.034. URL: http://www.sciencedirect.com/science/article/pii/S0301421510007202.

[48] Enterprise Surveys and The World Bank. *Data on Infrastructure - World Bank Enterprise Survey of Business Managers*. Survey. The World Bank Group, 2016. URL: http://www.enterprisesurveys.org.

[49] Pierluigi Mancarella and Gianfranco Chicco. "Global and Local Emission Impact Assessment of Distributed Cogeneration Systems with Partial-Load Models". In: *Applied Energy* 86.10 (Oct. 2009), pp. 2096–2106. ISSN: 03062619. DOI: 10.1016/j.apenergy.2008.12.026. URL: http://linkinghub.elsevier.com/retrieve/pii/S0306261908003516.

[50] V. S. K. Murthy Balijepalli, S. A. Khaparde, and C. V. Dobariya. "Deployment of MicroGrids in India". In: *IEEE PES General Meeting*. IEEE PES General Meeting. July 2010, pp. 1–7. DOI: 10.1109/PES.2010.5589956.

[51] Robert M. Cuzner and Giri Venkataramanan. "The Status of DC Micro-Grid Protection". In: *Industry Applications Society Annual Meeting, 2008. IAS'08. IEEE*. IEEE, 2008, pp. 1–8. URL: http://ieeexplore.ieee.org/xpls/abs_all.jsp?arnumber=4659170.

[52] Brian Fortenbery, Ecos Consulting EPRI, and William Tschudi. "DC Power for Improved Data Center Efficiency". In: *Lawrence Berkeley National Laboratory, University of California, California* (2008). URL: https://pdfs.semanticscholar.org/5268/2f8c38e24390fb9b392e61b7d3686ee4c196.pdf.

[53] D. J. Becker and B. J. Sonnenberg. "DC Microgrids in Buildings and Data Centers". In: *2011 IEEE 33rd International Telecommunications Energy Conference*. 2011 IEEE 33rd International Telecommunications Energy Conference. Oct. 2011, pp. 1–7. DOI: 10.1109/INTLEC.2011.6099725.

[54] Ahmed T. Elsayed, Ahmed A. Mohamed, and Osama A. Mohammed. "DC Microgrids and Distribution Systems: An Overview". In: *Electric Power Systems Research* 119 (Feb. 2015), pp. 407–417. ISSN: 0378-7796. DOI: 10.1016/j.epsr.2014.10.017. URL: http://www.sciencedirect.com/science/article/pii/S0378779614003885.

[55] Ishwari Tank and Shrikant Mali. "Renewable Based DC Microgrid with Energy Management System". In: *Signal Processing, Informatics, Communication and Energy Systems (SPICES), 2015 IEEE International Conference On*. IEEE, 2015, pp. 1–5. URL: http://ieeexplore.ieee.org/xpls/abs_all.jsp?arnumber=7091542.

[56] Md Junayed Sarker et al. "DC Micro-Grid with Distributed Generation for Rural Electrification". In: *2012 47th International Universities Power Engineering Conference (UPEC)*. IEEE, 2012, pp. 1–6. URL: http://ieeexplore.ieee.org/xpls/abs_all.jsp?arnumber=6398580.

[57] B. Alipuria et al. "Application of DC Micro-Grids for Integration of Solar Home Systems in Smart Grids". In: *Intelec 2013; 35th International Telecommunications Energy Conference, SMART POWER AND EFFICIENCY*. Intelec 2013; 35th International Telecommunications Energy Conference, SMART POWER AND EFFICIENCY. Oct. 2013, pp. 1–6.

[58] Yang Han et al. "Energy Management Method for Photovoltaic DC Micro-Grid System Based on Power Tracking Control". In: *IECON 2016 - 42nd Annual Conference of the IEEE Industrial Electronics Society*. IECON 2016 - 42nd Annual Conference of the IEEE Industrial Electronics Society. Oct. 2016, pp. 3058–3063. DOI: 10.1109/IECON.2016.7793868.

[59] Y. K. Chen et al. "Design and Implementation of Energy Management System With Fuzzy Control for DC Microgrid Systems". In: *IEEE Transactions on Power Electronics* 28.4 (Apr. 2013), pp. 1563–1570. ISSN: 0885-8993. DOI: 10.1109/TPEL.2012.2210446.

[60] Ali Bidram and Ali Davoudi. "Hierarchical Structure of Microgrids Control System". In: *IEEE Transactions on Smart Grid* 3.4 (Dec. 2012), pp. 1963–1976. ISSN: 1949-3053. DOI: 10.1109/TSG.2012.2197425. URL: http://ieeexplore.ieee.org/document/6202752/.

[61] T. L. Vandoorn et al. "Microgrids: Hierarchical Control and an Overview of the Control and Reserve Management Strategies". In: *IEEE Industrial Electronics Magazine* 7.4 (Dec. 2013), pp. 42–55. ISSN: 1932-4529. DOI: 10.1109/MIE.2013.2279306.

[62] Ashray Manur. "Microgrid Energy Management System". Masters Thesis. University of Wisconsin-Madison, 2015. URL: https://minds.wisconsin.edu/handle/1793/73976.

[63] Dong Chen, Lie Xu, and Liangzhong Yao. "DC Voltage Variation Based Autonomous Control of DC Microgrids". In: *IEEE Transactions on Power Delivery* 28.2 (Apr. 2013), pp. 637–648. ISSN: 0885-8977. DOI: 10.1109/TPWRD.2013.2241083. URL: http://ieeexplore.ieee.org/lpdocs/epic03/wrapper.htm?arnumber=6449332.

[64] Chi Jin et al. "Implementation of Hierarchical Control in DC Microgrids". In: *IEEE Transactions on Industrial Electronics* 61.8 (Aug. 2014), pp. 4032–4042. ISSN: 0278-0046, 1557-9948. DOI: 10.1109/TIE.2013.2286563. URL: http://ieeexplore.ieee.org/lpdocs/epic03/wrapper.htm?arnumber=6642055.

[65] Vahidreza Nasirian et al. "Distributed Cooperative Control of DC Microgrids". In: *IEEE Transactions on Power Electronics* 30.4 (Apr. 2015), pp. 2288–2303. ISSN: 0885-8993. DOI: 10.1109/TPEL.2014.2324579. URL: http://ieeexplore.ieee.org/lpdocs/epic03/wrapper.htm?arnumber=6816073.

[66] Sandeep Anand, Baylon G. Fernandes, and Josep Guerrero. "Distributed Control to Ensure Proportional Load Sharing and Improve Voltage Regulation in Low-Voltage DC Microgrids". In: *IEEE Transactions on Power Electronics* 28.4 (Apr. 2013), pp. 1900–1913. ISSN: 0885-8993. DOI: 10.1109/TPEL.2012.2215055. URL: http://ieeexplore.ieee.org/lpdocs/epic03/wrapper.htm?arnumber=6287047.

[67] P. J. Hart, R. H. Lasseter, and T. M. Jahns. "Symmetric Droop Control for Improved Hybrid AC/DC Microgrid Transient Performance". In: *2016 IEEE Energy Conversion Congress and Exposition (ECCE)*. 2016 IEEE Energy Conversion Congress and Exposition (ECCE). Sept. 2016, pp. 1–8. DOI: 10.1109/ECCE.2016.7855486.

[68] Poh Chiang Loh et al. "Hybrid AC & DC Microgrids With Energy Storages and Progressive Energy Flow Tuning". In: *IEEE Transactions on Power Electronics* 28.4 (Apr. 2013), pp. 1533–1543. ISSN: 0885-8993. DOI: 10.1109/TPEL.2012.2210445. URL: http://ieeexplore.ieee.org/lpdocs/epic03/wrapper.htm?arnumber=6249790.

[69] Q. Shafiee et al. "Hierarchical Control for Multiple DC-Microgrids Clusters". In: *IEEE Transactions on Energy Conversion* 29.4 (Dec. 2014), pp. 922–933. ISSN: 0885-8969. DOI: 10.1109/TEC.2014.2362191.

[70] P. Tian et al. "A Hierarchical Energy Management System Based on Hierarchical Optimization for Microgrid Community Economic Operation". In: *IEEE Transactions on Smart Grid* 7.5 (Sept. 2016), pp. 2230–2241. ISSN: 1949-3053. DOI: 10.1109/TSG.2015.2470551.

[71] Ashray Manur et al. "MEM: Energy Management System for Low Voltage DC Microgrids". In: *Sustainable Green Buildings and Communities*. Sustainable Green Buildings and Communities. Chennai, India, 2016 (forthcoming).

[72] SGBC. *First International Conference on Sustainable Green Buildings & Communities Conference*. 2016. URL: http://www.sgbcconf.org/.

[73] Adria E. Brooks, Ashray Manur, and Giri Venkataramanan. "Energy Modeling of Aggregated Community Scale Residential Microgrids". In: *Sustainable Green Buildings and Communities*. Sustainable Green Buildings and Communities. Chennai, India, 2016 (forthcoming).

[74] Ashray Manur and Giri Venkataramanan. "Wireless Sensor Network for DC/AC Homegrids". In: *Sustainable Green Buildings and Communities*. Sustainable Green Buildings and Communities. Chennai, India, 2016 (forthcoming).

[75] NXP Semiconductors. *I2C-Bus Specification and User Manual*. Apr. 4, 2014. URL: http://www.nxp.com/documents/user_manual/UM10204.pdf.

[76] Linear Technology. *LTC2946 Wide Range I2C Power, Charge and Energy Monitor*. 2014. URL: http://www.linear.com/LTC2946.

[77] K.C. Divya and Jacob Østergaard. "Battery Energy Storage Technology for Power Systems—An Overview". In: *Electric Power Systems Research* 79.4 (Apr. 2009), pp. 511–520. ISSN: 03787796. DOI: 10.1016/j.epsr.2008.09.017. URL: http://linkinghub.elsevier.com/retrieve/pii/S0378779608002642.

[78] Rodolfo Dufo-López, Juan M. Lujano-Rojas, and José L. Bernal-Agustín. "Comparison of Different Lead–acid Battery Lifetime Prediction Models for Use in Simulation of Stand-Alone Photovoltaic Systems". In: *Applied Energy* 115 (Feb. 15, 2014), pp. 242–253. ISSN: 0306-2619. DOI: 10.1016/j.apenergy.2013.11.021. URL: http://www.sciencedirect.com/science/article/pii/S0306261913009148.

[79] B. Zhao et al. "Operation Optimization of Standalone Microgrids Considering Lifetime Characteristics of Battery Energy Storage System". In: *IEEE Transactions on Sustainable Energy* 4.4 (Oct. 2013), pp. 934–943. ISSN: 1949-3029. DOI: 10.1109/TSTE.2013.2248400.

[80] Kathryn R. Bullock. "Lead/Acid Batteries". In: *Journal of power sources* 51 (1-2 1994), pp. 1–17. URL: http://www.sciencedirect.com/science/article/pii/0378775394019525.

[81] Nirmal-Kumar C. Nair and Niraj Garimella. "Battery Energy Storage Systems: Assessment for Small-Scale Renewable Energy Integration". In: *Energy and Buildings* 42.11 (Nov. 2010), pp. 2124–2130. ISSN: 0378-7788. DOI: 10.1016/j.enbuild.2010.07.002. URL: http://www.sciencedirect.com/science/article/pii/S0378778810002185.

[82] Elena M. Krieger, John Cannarella, and Craig B. Arnold. "A Comparison of Lead-Acid and Lithium-Based Battery Behavior and Capacity Fade in off-Grid Renewable Charging Applications". In: *Energy* 60 (Oct. 1, 2013), pp. 492–500. ISSN: 0360-5442. DOI: 10.1016/j.energy.2013.08.029. URL: http://www.sciencedirect.com/science/article/pii/S0360544213007044.

[83] M. Armand and J.-M. Tarascon. "Building Better Batteries". In: *Nature* 451.7179 (Feb. 7, 2008), pp. 652–657. ISSN: 0028-0836. DOI: 10.1038/451652a. URL: http://www.nature.com.ezproxy.library.wisc.edu/nature/journal/v451/n7179/full/451652a.html.

[84] Boucar Diouf and Ramchandra Pode. "Potential of Lithium-Ion Batteries in Renewable Energy". In: *Renewable Energy* 76 (Apr. 2015), pp. 375–380. ISSN: 0960-1481. DOI: 10.1016/j.renene.2014.11.058. URL: http://www.sciencedirect.com/science/article/pii/S0960148114007885.

[85] Shuo Pang et al. "Battery State-of-Charge Estimation". In: *American Control Conference, 2001. Proceedings of the 2001*. American Control Conference, 2001. Proceedings of the 2001. Vol. 2. 2001, 1644–1649 vol.2. DOI: 10.1109/ACC.2001.945964.

[86] Sabine Piller, Marion Perrin, and Andreas Jossen. "Methods for State-of-Charge Determination and Their Applications". In: *Journal of Power Sources*. Proceedings of the 22nd International Power Sources Symposium 96.1 (June 1, 2001), pp. 113–120. ISSN: 0378-7753. DOI: 10.1016/S0378-7753(01)00560-2. URL: http://www.sciencedirect.com/science/article/pii/S0378775301005602.

[87] M. Coleman et al. "State-of-Charge Determination From EMF Voltage Estimation: Using Impedance, Terminal Voltage, and Current for Lead-Acid and Lithium-Ion Batteries". In: *IEEE Transactions on Industrial Electronics* 54.5 (Oct. 2007), pp. 2550–2557. ISSN: 0278-0046. DOI: 10.1109/TIE.2007.899926.

[88] G L Shekar. *Farewell to Dr. Venkata Giri Venkataramanan*. May 13, 2015. URL: http://www.nie.ac.in/wp-content/uploads/2015/11/circular_0012.pdf.

[89] Editor. *NIE Signs MoU with University of Wisconsin-Madison*. June 3, 2016. URL: http://citytoday.news/nie-signs-mou-with-university-of-wisconsin-madison/.

[90] NREL. *PVWatts Calculator Version 5.3.8 (India)*. Oct. 2016. URL: http://pvwatts.nrel.gov/India/index.php.

[91] India Meteorological Department. *District-Wise Monthly Rainfall Data, List of Raingauge Stations*. Sept. 1, 2012. URL: http://www.indiawaterportal.org/articles/district-wise-monthly-rainfall-data-list-raingauge-stations-india-meteorological-department.

[92] Solarex. *Millenia Photovoltaic Modules*. 1999.

[93] Andreas Wagner. *Photovoltaik Engineering: Handbuch für Planung, Entwicklung und Anwendung*. Springer-Verlag, Nov. 27, 2015. 476 pp. ISBN: 978-3-662-48640-5.

[94] Bruce Mulliken. "Solarex Fades Away". In: *Green Energy News* (Mar. 27, 2010). URL: http://www.green-energy-news.com/arch/nrgs2010/20100020.html.

[95] Kevin Bullis. "Why BP Solar Failed". In: *MIT Technology Review* (Dec. 21, 2011). URL: https://www.technologyreview.com/s/426461/why-bp-solar-failed/.

[96] Bhubaneswari Parida, S. Iniyan, and Ranko Goic. "A Review of Solar Photovoltaic Technologies". In: *Renewable and Sustainable Energy Reviews* 15.3 (Apr. 2011), pp. 1625–1636. ISSN: 1364-0321. DOI: 10.1016/j.rser.2010.11.032. URL: http://www.sciencedirect.com/science/article/pii/S1364032110004016.

[97] NREL. *Cell Efficiency Explanatory Notes*. Explanatory Notes. Golden, CO (US): National Renewable Energy Laboratory, 2016. URL: https://www.nrel.gov/pv/.

[98] Martin A. Green et al. "Solar Cell Efficiency Tables (Version 49)". In: *Progress in Photovoltaics: Research and Applications* 25.1 (Jan. 2017), pp. 3–13. ISSN: 10627995. DOI: 10.1002/pip.2855. URL: http://doi.wiley.com/10.1002/pip.2855.

[99] D. C. Jordan and S. R. Kurtz. "Photovoltaic Degradation Rates—an Analytical Review". In: *Progress in Photovoltaics: Research and Applications* 21.1 (Jan. 1, 2013), pp. 12–29. ISSN: 1099-159X. DOI: 10.1002/pip.1182. URL: http://onlinelibrary.wiley.com.ezproxy.library.wisc.edu/doi/10.1002/pip.1182/abstract.

[100] Kirloskar Oil Engines Limited. *Kirloskar Chhota Chilli*. 2017. URL: http://www.koelgreen.com/3-kva-5-kva.

[101] Primus Wind Power. *Air X Turbine*. 2013. URL: http://www.primuswindpower.com/wind-power-products/air-30-turbine-2/.

[102] Roberto Faranda and Sonia Leva. "Energy Comparison of MPPT Techniques for PV Systems". In: *WSEAS transactions on power systems* 3.6 (2008), pp. 446–455. URL: http://www.wseas.us/e-library/transactions/power/2008/27-545.pdf.

[103] M. A. G. de Brito et al. "Evaluation of the Main MPPT Techniques for Photovoltaic Applications". In: *IEEE Transactions on Industrial Electronics* 60.3 (Mar. 2013), pp. 1156–1167. ISSN: 0278-0046. DOI: 10.1109/TIE.2012.2198036.

[104] Phocos. *MPPT 100/30 Datasheet*. Oct. 17, 2013. URL: http://www.phocos.co.in/products/mppt-100-30a.

[105] Kaushiki Sanyal. *The Scheduled Tribes (Recognition of Forest Rights) Bill, 2005*. Legislative Brief. New Delhi, India: Parliamentary Research Service, Apr. 6, 2006. URL: http://www.prsindia.org/uploads/media/1167469383/legis1167477829_legislative_brief_scheduled_tribes_bill.pdf.

[106] Sharachchandra Lélé. "A 'Defining' Moment for Forests?" In: *Economic and Political Weekly* 42.25 (2007), pp. 2379–2383. ISSN: 0012-9976. URL: http://www.jstor.org.ezproxy.library.wisc.edu/stable/4419725.

[107] Nayantara Narayanan. *A Short History of India's Two-Decade Struggle to Define What a Forest Actually Is*. May 12, 2015. URL: https://scroll.in/article/726461/a-short-history-of-indias-two-decade-struggle-to-define-what-a-forest-actually-is.

[108] K. N. Chaturvedi. *The Scheduled Tribes and Other Traditional Forest Dwellers (Recogniction of Forest Rights) Act*. Dec. 29, 2006. URL: http://extwprlegs1.fao.org/docs/pdf/ind77867.pdf.

[109] Balachandran Chidambaranatraj. *Construction of Environment & Child Friendly (E&CF) Anganawadi Centres with GBC (Green Building Concept) Approach - in the Midst of Mysore Range Forest Tribal Area*. Project Report. Mysuru, India: CREST, Mar. 27, 2016.

[110] *THE BAMBOO SCHOOL: A Documentary on Eco Sensitive Anganwadi Kendra*. Aug. 20, 2016. URL: https://vimeo.com/179607063.

[111] H.N. Narasimha Kumar. "An All-Bamboo Anganwadi in the Forest". In: *The Hindu* (Mar. 27, 2016). URL: http://www.thehindu.com/news/national/karnataka/an-allbamboo-anganwadi-in-the-forest/article8400831.ece.

[112] Bosch Limited. *Bosch India Foundation*. 2017. URL: http://www.boschindia.com/en/in/sustainability_innovation_5/bosch_india_csr_bif.html.